Chapter 3

Synthesis and study of dithienopyrrolo benzothiadiazole (DTPBT) -isoindigo based conjugated polymers and their SCLC hole mobilities

Table of contents

Introduction **86**

Results and discussion **93**

Synthesis of monomers and polymers 93

Molecular weight and thermal properties of polymers 96

Photophysical properties of monomer 97

Photophysical properties of polymer 98

Electrochemical properties of monomer 99

Electrochemical properties of polymers 100

Computational studies 103

Device fabrication and characterization 105

Conclusion **109**

Experimental procedures **110**

General procedure 110

Synthesis of 5-bromo-1-(2-ethylhexyl)indolin-2-one 110

Synthesis of 10,11-bis(2-ethylhexyl)-10,11-dihydro-[*1,2,5*]thiadiazolo[*3,4-e*]thieno[*2',3':4,5*]pyrrolo[*3,2-g*]thieno[*3,2-b*]indole-2,8-dicarbaldehyde 111

Synthesis of monomer 115

Synthesis of (Z)-5-bromo-3-((4-((2-((Z)-5-bromo-1-(2-ethylhexyl)-2-oxoindolin-3-ylidene)ethyl)thio)-6,7-bis(2-ethylhexyl)-6,7-dihydropyrrolo[3,2-g] [1,2,5] thiadiazolo[3,4-e]thieno[3,2-b]indol-9-yl)methylene)-1-(2-ethylhexyl)indolin-2-one **(DTPBT-IIG)** 115

Synthesis of polymer 115

General procedure for synthesis of DTPBT based conjugated polymers **DTPBT-BTP**, **DTPBT-FTP** and **DTPBT-TP** 116

Spectral data 117

References 127

Introduction

The field of conjugated polymers has witnessed substantial growth and attention in recent decades, particularly in the context of their applications in various electronic and optoelectronic devices. Conjugated polymers are a class of polymers with alternating single and double bonds along their backbone, leading to a delocalized π-electron system. This unique structure imparts them with intriguing electronic and optical properties, making them attractive for a range of applications. Conjugated polymers have been extensively studied for use in OFETs.[1–3] OFETs are fundamental building blocks for flexible and low-cost electronic devices. The ability of conjugated polymers to conduct charge carriers and their compatibility with flexible substrates make them suitable for these applications.[4,5] Electrochromic devices undergo reversible colour changes in response to an applied voltage.[6] Conjugated polymers are used in electrochromic materials due to their ability to change their absorption properties in response to an electric field. This property is utilized in smart windows, displays and other applications.[7] Conjugated polymers play a crucial role in organic photovoltaic cells, also known as organic solar cells. These cells convert sunlight into electricity using organic semiconductors, and conjugated polymers are employed as the active material in the photoactive layer.[8] OLEDs are used in displays and lighting applications. Conjugated polymers with luminescent properties are utilized as emissive materials in OLEDs.[9,10] Their ability to emit light efficiently and in various colours contributes to the vibrant displays seen in modern electronic devices.[11]

The advantages of using conjugated polymers in these applications include their tunable electronic properties, ease of processing into thin films and potential for solution-based fabrication methods, which can be cost-effective and compatible with large-scale manufacturing processes. Researchers continue to explore new conjugated polymer materials, improved processing techniques and novel device architectures to enhance the performance and broaden the scope of applications in the field of organic electronics.[12] The superior electronic properties can be achieved by suitable combination of molecular design, processing technology and device construction.[13,14] Various conjugated polymer materials with improved performance, such as higher charge carrier mobility, better stability and increased absorption efficiency have been a focus of research in the field of organic electronics.[8,15]

The conducting, luminescent, and sensing capabilities of thiophene-based oligomers and polymers have attracted a lot of attention in the field of material science, particularly in the organic electronic domain.[16–18] There are two main reasons why polythiophenes are so dominant in the *p*-conjugated polymer industry.[19,20] In the several conjugated materials used in organic electronics, thiophene and its derivatives are well-known donors.

The functionalization of the core thiophene units has been achieved by a variety of synthetic approaches.[17,21,22] In the last 20 years, the development of transition metal catalysed cross-coupling processes has led to the discovery of several important thiophene-based scaffolds, which have made it possible to tune the optical and electrical characteristics of the resulting polymers and polymer-based materials. The exceptional chemical and physical properties of the polythiophene are the second explanation. Polythiophene has excellent thermal and chemical stability together with strong conductivity.[23] The stacking configuration and self-assembly on bulk and solid surfaces produced these special qualities.[18,24]

The tuneable features and activities of donor-acceptor (D-A) polymers, which are synthesised by integrating ladder-type conjugated molecules, have garnered substantial attention in recent times.[25] These polymers are made up of ladder-type small conjugated molecules that are created by combining aromatic and heterocyclic building blocks with low electron density (like benzothiadiazole, thieno-pyrrolodione, bithiopheneimide, quinoxaline, naphthobisthiadiazole, diketopyrrolopyrrole, thiazolothiazole, dithienopyrrolobenzothiadiazole, etc.) and/or electron-rich building blocks (like furan, benzene, thiophene, selenophene, pyrrole, silole, germole, cyclopentadiene.[26–29]

Dithienopyrrolobenzothiadiazole (DTPBT) is a well-known ladder-type conjugated molecule that has demonstrated intriguing optical and electronic properties. [30,31] It is composed of an electron-deficient 2,1,3-benzothiadiazole (BT) unit that can fuse with two electron-rich thiophene units through two embedded pyrrole rings (Figure 3.1). Additionally, DTPBT-based polymers have good charge transport characteristics, making them suitable for use in organic solar cells, organic field-effect transistors, and organic light-emitting diodes. DTPBT unit, as a coplanar ladder-type heteroarenes, has been used as an effective acceptor unit to build D–A copolymers for photovoltaic applications.[32]

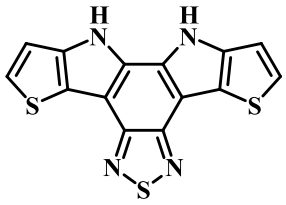

Figure 3.1 structure of D-A type dithienopyrrolobenzothiadiazole (**DTPBT**)

Dithienopyrrolobenzothiadiazole-Carbazole based D-π-A-π-D type conjugated molecule was reported by kadam *et al.*[33](Figure 3.2) This compound was synthesized by Wittig reaction of carbazole Wittig salt and diformyl dioctyl ditheniopyrrolobenzothiadiazole. The measured space-charge limited current (SCLC) hole mobility for the synthesised compound was found to be 3.85×10^{-4} $cm^2V^{-1}s^{-1}$ which showed that combining ditheniopyrrolobenzothiadiazole with the electron-rich unit such as carbazole can be a viable strategy to create a good hole-transporting materials (HTMs).

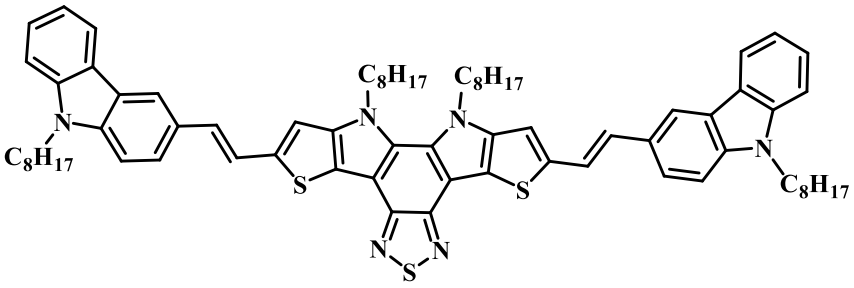

Figure 3.2 Dithienopyrrolobenzothiadiazole (DTPBT)-Carbazole based D-π-A-π-D type conjugated molecule reported by kadam *et al.*[33]

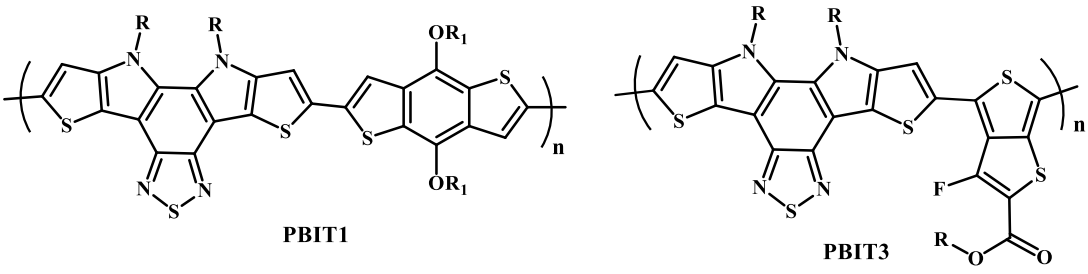

PBIT1 **PBIT3**

Figure 3.3 Structures of DTPBT based D-A type conjugated polymers reported by Carsten *et al.* [13]

Carsten *et al.*[34] reported two novel DTPBT-based conjugated polymers with 4,8-bis(2-butyloctyloxy) benzo[1,2-*b*:4,5-*b'*]dithiophene and 2-ethylhexyl 3-fluorothieno[3,4-*b*]thiophene-2-carboxylate *via* Stille coupling reaction (Figure 3.3).

These two low band gap polymers with different structures, energy bandgaps and levels were used to prepare BHJ solar cells. The SCLC hole mobilities of these two polymers are 3.43 X 10^{-4} and 2.95 X 10^{-4} $cm^2V^{-1}s^{-1}$, respectively.

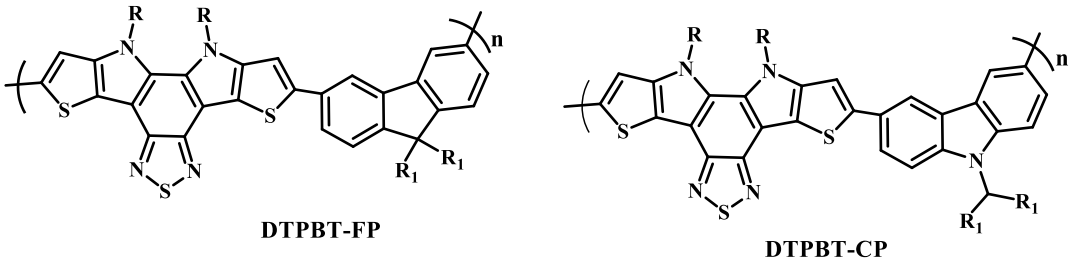

Figure 3.4 Structure of DTPBT based D-A type conjugated polymers reported by Cheng *et al.* [35]

Cheng *et al.* [35] reported DTPBT based D-A type conjugated polymers with fluorene and carbazole unit. The polymerization was carried out by Suzuki and Stille polymerization reaction (Figure 3.4). The SCLC hole mobilities of these synthesized polymers are observed at 4.7 X 10^{-5} and 1.8 X 10^{-5} $cm^2V^{-1}s^{-1}$, respectively.

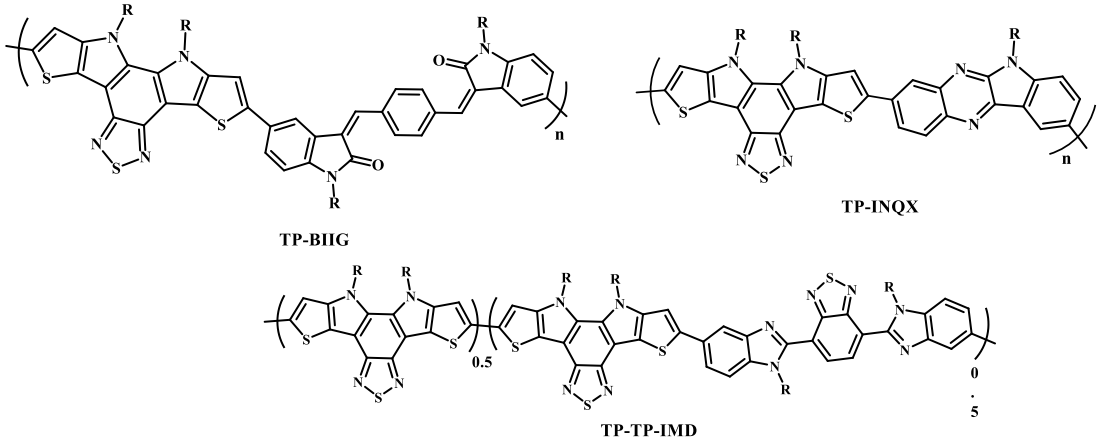

Figure 3.5 Structure of DTPBT based D-A type conjugated polymers reported by Bhanvadia *et al.* [36]

Bhanvadia *et al.*[36] reported donor-acceptor integrated ladder-type DTPBT-based conjugated polymers. Polymers show $\pi-\pi$ stacks promoted high SCLC hole mobilities ranging between 5.6×10^{-4} –1.3×10^{-3} $cm^2V^{-1}s^{-1}$(Figure 3.5). The obtained SCLC hole mobility data in tandem with the studied structural aspects of monomers and morphological aspects of polymers, suggest that the combination of ladder-type DTPBT-scaffolds (capable of intermolecular π–π interactions) with non-ladder-type

planar and structurally rigid π extended conjugated scaffolds (capable of intermolecular $\pi-\pi$ and other non-bonding interactions) is beneficial for getting good hole mobilities. The polymers exhibit moderate to good visible light absorptivity with HOMO energy levels below −5.0 eV, according to the analysis of their photophysical and electrochemical characteristics. According to X-ray diffraction experiments, polymers TP-BIIG, TP-INQX, and TP-TP-IMD preferentially align their polymer chains face-on with regard to the substrate.

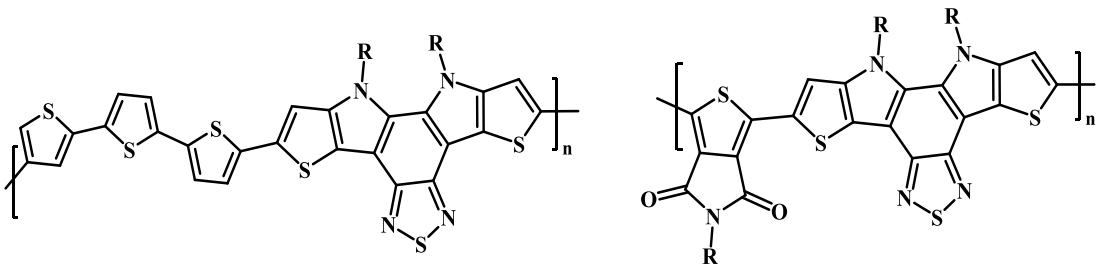

PTTPBT PTPDPBT

Figure 3.6 Structure of DTPBT based D-A type conjugated polymers reported by Kadam *et al.*[37]

Kadam *et al.*[37] synthesized two distinct *p*-type donor–acceptor DTPBT-based conjugated polymers by Suzuki and Stille coupling was used to carry out the chemical polymerization (Figure 3.6). The optical bandgap of the polymers, PTTPBT and PTPDPBT were found to be at 2.1 eV, and 1.9 eV, respectively. The observed hole mobility for polymers, PTTPBT and PTPDPBT, using the SCLC technique, was 2.36 x 10^4 cm^2 V^1 s^1, and 2.18 x 10^4 cm^2 V^1 s^1, respectively. The synthesized polymers have high thermal stabilities for use in optoelectronic applications are demonstrated by their decomposition temperatures, which are over 200 ℃. The obtained results indicate that these polymers have a potentilal as *p*-type polymer semiconductors.

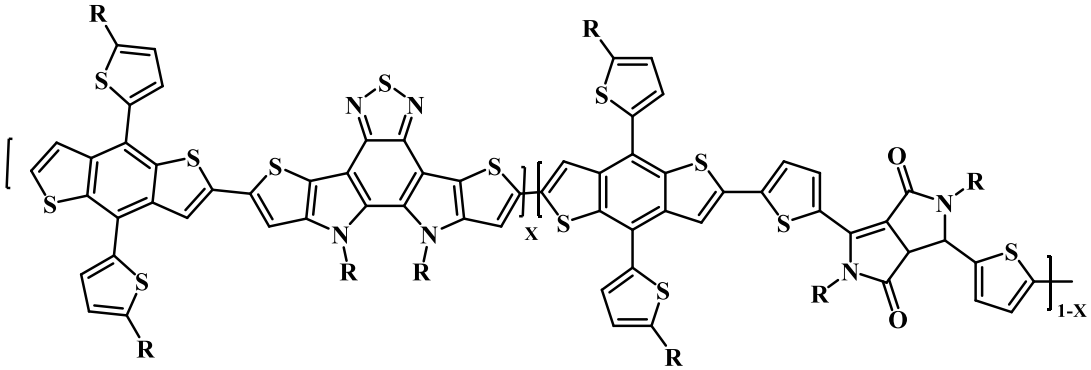

PBDT-D30-T70, X=0.7
PBDT-D70-T30, X=0.3
R=2ethylhexyl

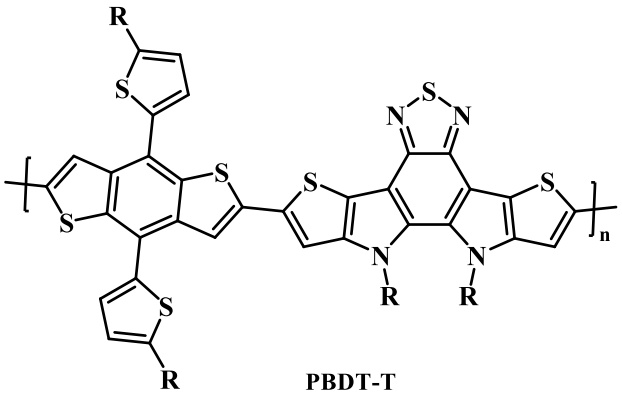

Figure 3.7 Structure of DTPBT-based D-A type conjugated polymers reported by Yong *et al.*[15]

Yong *et al.* [15] synthesized and characterized two random terpolymers (PBDT-D70-T30 and PBDT-D30-T70) based on dithienopyrrolobenzothiadiazole (TPBT) and a parent D-A copolymer (PBDT-T)(Figure 3.7). The terpolymers have electron-deficient TPBT and diketopyrrolopyrrole (DPP) moieties conjugated with random alternating benzodithiophene (BDT) units that exhibit complementary light absorption behaviour. In comparison to the original copolymer, the terpolymers had wider absorption bands, lower lying HOMO energy levels, and better hole mobilities. Because of its wider light absorption and increased hole mobility, PBDT-D70-T30, which has a 70:30 ratio between DPP and TPBT, showed an enhanced power conversion efficiency (PCE) of 4.31%, a higher low short-circuit current density (*Jsc*) of 11.91 mA cm^{-2}, and a higher fill factor (FF) of 0.52. When compared to PBDT-D30-T70 (3.10%) and PBDT-D70-T30 (4.31%), the binary parent polymer PBDT-T yielded a PCE of 1.86%, showing a considerable decrease in PCE, which shows that improving the composition of random terpolymers is crucial to maximising PSC performance. Designing and synthesising new random terpolymers by incorporating two acceptor units with different electron-withdrawing strengths is a promising and efficient method of increasing the absorption and improving the charge mobility of the parent polymer.

electron-deficient isoindigo derivatives as acceptors in donor-acceptor (D-A) type copolymers, highlighting their excellent semiconducting properties π-extended isoindigo derivatives, acting as electron-withdrawing building blocks, have been synthesized by connecting isoindigo units to various conjugated units on both sides.[38–40]

In organic electronics, such as organic photovoltaics (OPVs) or organic field-effect transistors (OFETs), D-A copolymers are commonly employed.[38] In these systems, the electron-deficient component (acceptor) and the electron-rich component (donor) work together to facilitate charge transfer and improve the overall electronic performance of the material.[16,41,42]

The electron-deficient isoindigo derivatives have been used as an acceptor in D-A-type copolymers which showed excellent semiconducting properties.[43,44] Its electron-deficient nature makes it suitable for acting as an acceptor in D-A systems.[45] By covalently linking isoindigo units to conjugated units, the resulting π-extended isoindigo derivatives likely enhance the electronic interactions within the material, potentially leading to improved charge transport properties.[46,47]

Higher space charge current mobility seen in conjugated polymers based on π-extended DTPBT-isoindigo, which enhances charge transfer efficiency, can be attributed to the planar structure of DTPBT. π-extended isoindigo derivatives also offer significant intramolecular charge transfer (ICT) and favourable π-π interactions.[48,49] In summary, the combination of a planar structure in DTPBT and the isoindigo unit in the conjugated polymers showed improved charge transport properties, elevated SCLC mobility, strong ICT and favourable π-π interactions, making them promising material for applications in electronic devices.[29]

Results and discussion

Synthesis of monomers and polymers

The 5-bromo-1-(2-ethylhexyl) indolin-2-one (**2**) is synthesized according to the reported literature process (Scheme 3.1). 5-Bromoisatin is subjected to *n*-alkylation using potassium carbonate (K_2CO_3) and 2-ethylhexyl bromide. The resulting compound **1** is subjected to Wolff-Kishner type reaction using hydrazine hydrate. [50–52]

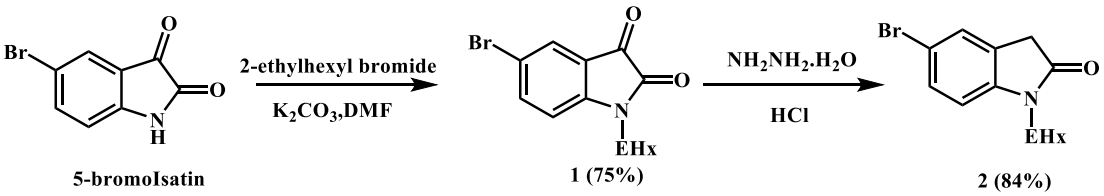

Scheme 3.1 Synthesis of 5-bromo-1-(2-ethylhexyl) indolin-2-one (**2**)

Compound **3** and compound **4** are synthesized according to the literature procedures.[46,53] Compound **5** is prepared from compound **4** using nitronium trifluoromethanesulfonate (NTMS) as a nitrating agent according to the literature procedure reported by Wang *et al.*[11] Compound **6** is synthesized by Stille coupling reaction between compound **5** and 2-(tri-*n*-butylstannyl)thiophene in dry THF using $Pd(PPh_3)_2Cl_2$ as a catalyst under nitrogen atmosphere using literature procedure.[54] Compound **7** is synthesized by Cadogan intramolecular annulation according to the literature procedure reported by Kato *et al.*[55] Alkylation of compound **7** was carried out by using 2-ethylhexyl bromide in presence of NaOH and DMF. The formylation of synthesised compound **8** was carried out by phosphrous oxychloride ($POCl_3$) and dimethyl formamide (DMF) to form compound **9** (Scheme 3.2).

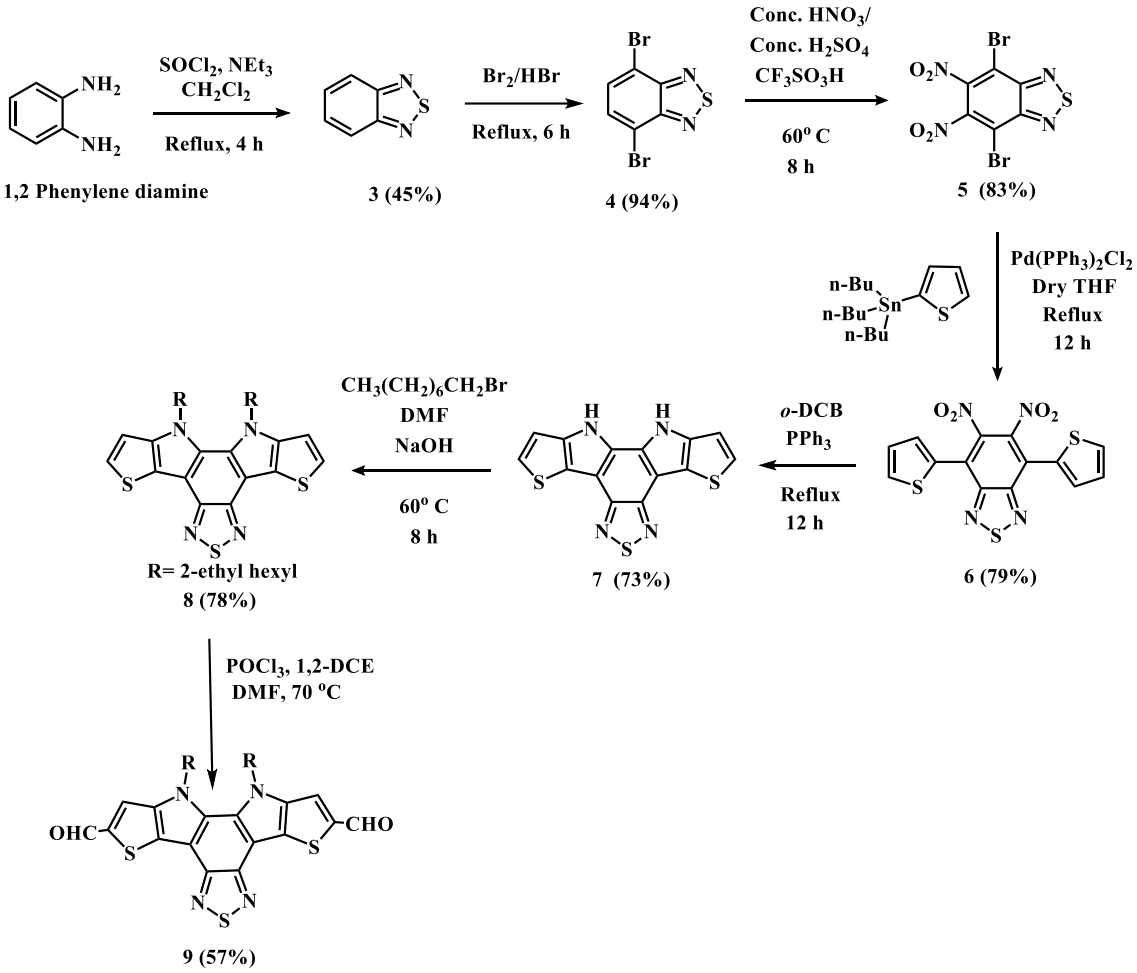

Scheme 3.2 Synthesis of 10,11-bis(2-ethylhexyl)-10,11-dihydro-[1,2,5]thiadiazolo [3,4-e]thieno[2',3':4,5]pyrrolo[3,2-g]thieno[3,2-b]indole-2,8-dicarbaldehye.

π-Extended DTPBT-isoindigo based compound **DTPBT-IIG** was synthesised by Knoevenagel condensation reaction between compound **9** with 2-ethylhexylindoline-2-one (**2**) in presence of piperidine in acetonitrile/chloroform solvent system.

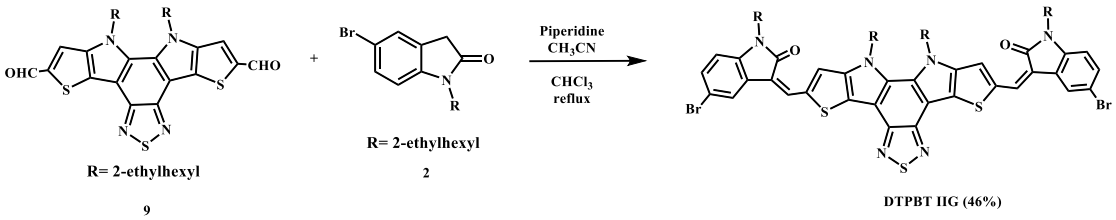

Scheme 3.3 Synthesis of compound **DTPBT-IIG**

Donor-acceptor type π-extended DTPBT based conjugated polymers were synthesised *via* Stille coupling reaction (Scheme 3.4). Polymers, **DTPBT-BTP**, **DTPBT-FTP** and **DTPBT-TP** were synthesized by treating compound **DTPBT-IIG** with 5,5'-

bis(trimethylstannyl)2-2'-bithiophene, 2,5-bis(trimethylstannyl)thieno[3,2-*b*] thiophene and 2,5-bis(trimethylstannyl)thiophene, respectively in presence of $Pd_2(dba)_3$ catalyst and tri-*o*-tolyl phosphine in toluene. The resulting polymers were purified by Soxhlet extraction technique using methanol, petroleum ether, toluene and chloroform.

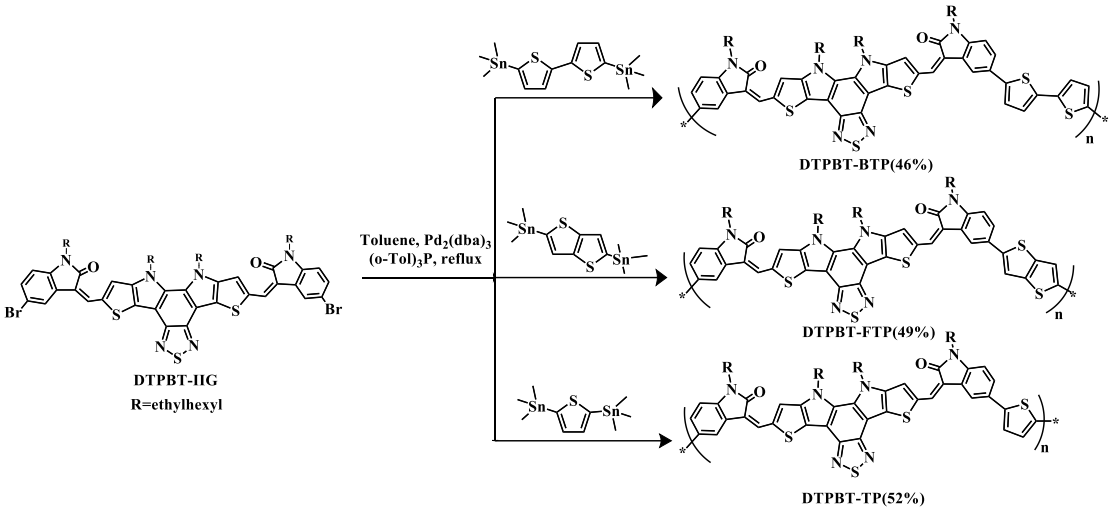

Scheme 3.4 Synthesis of π-extended D-A-type conjugated polymers, **DTPBT-BTP**, **DTPBT-FTP** and **DTPBT-TP**

Molecular weight and thermal properties of polymers

The decomposition temperature (T_d), average molecular weights (M_n and M_w) and poly dispersity index (PDI) of all synthesised conjugated polymers, **DTPBT-BTP**, **DTPBT-FTP** and **DTPBT-TP** were summarised in Table 3.1. The average molecular weight of polymers was calculated by gel permeation chromatography (GPC) analysis. The data obtained from GPC analysis indicates that the chain length of polymers were 12, 10 and 10 comonomer units for polymers, **DTPBT-BTP**, **DTPBT-FTP** and **DTPBT-TP** respectively.

Thermal properties of all the polymers were measured by thermo gravimetric analysis (TGA) at heating rate of 10 °C/min under nitrogen atmosphere. The decomposition temperature was defined as the temperature at which the compound loses 5% of its weight. The decomposition temperature for the polymers, **DTPBT-BTP**, **DTPBT-FTP** and **DTPBT-TP** were found to be 350 °C, 294 °C and 353 °C, respectively. The high decomposition temperature indicate that all the polymers showed a good thermal stability and are found suitable for an application in organic electronic devices.

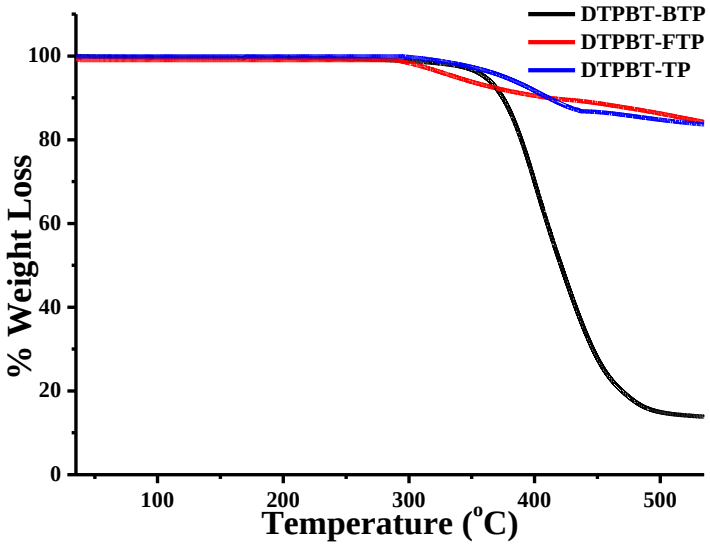

Figure 3.8 Thermogravimetric analysis (TGA) of DTPBT-isoindigo based conjugated polymers **DTPBT-BTP** (Black line), **DTPBT-FTP** (Red line) and **DTPBT-TP** (Blue line)

Photophysical properties of monomer

The photophysical properties of synthesised monmoner **DTPBT-IIG** was studied by UV-visible spectroscopy in a dilute chloroform solution. **DTPBT-IIG** showed multiple band absorption spectra with the complex band splitting patterns. As shown in Figure 3.9, the absorption spectra of **DTPBT-IIG** exhibit relatively broader first absorption band corresponding to the π-π* transitions, having absorption maxima (λ_{max}) at 351 nm. **DTPBT-IIG** showed a shoulder peak at 546 nm and the second band in the absorption spectrum with absorption maximum (λ_{max}) at 580 nm which can be due to the charge transfer (CT) transitions.

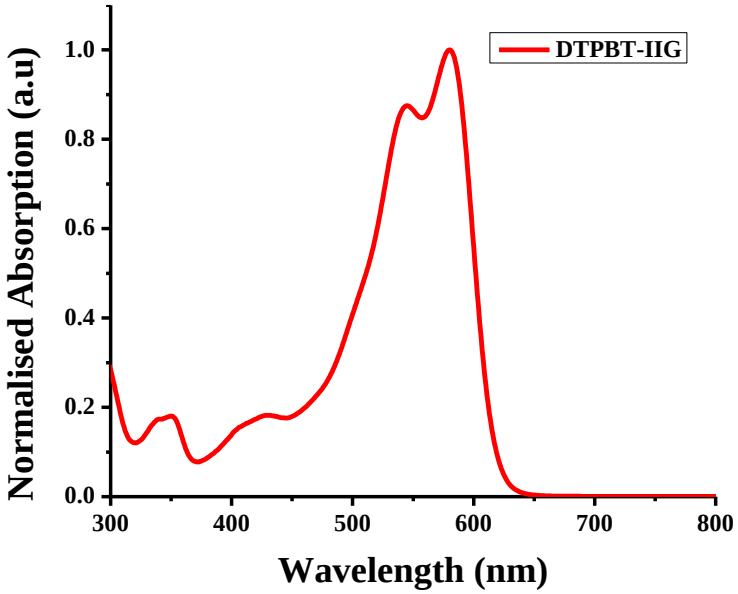

Figure 3.9 Absorption spectra of **DTPBT-IIG**

Photophysical properties of polymer

All three polymers, **DTPBT-BTP**, **DTPBT-FTP** and **DTPBT-TP** exhibit broad absorption spectra attributed to π-π* transitions (Figure 3.10). The absorption bands (λ_{max}) for polymers, **DTPBT-BTP**, **DTPBT-FTP** and **DTPBT-TP** are 353 nm, 351 nm, and 403 nm, respectively. The first absorption band of polymers, **DTPBT-BTP** and **DTPBT-TP** shows a shoulder peak at 374 nm and 355 nm, respectively. Polymer **DTPBT-BTP** shows a second absorption band at 583 nm, due to intramolecular charge transfer (ICT). Polymer **DTPBT-FTP** exhibits a similar ICT band at 553 nm, and **DTPBT-TP** at 555 nm. Shoulder peaks for ICT transition bands are observed at 580 nm, 585 nm, and 582 nm for polymers, **DTPBT-BTP**, **DTPBT-FTP** and **DTPBT-TP**, respectively. The absorption edge (λ_{edge}), are found at 661 nm, 667 nm, and 666 nm for polymers, **DTPBT-BTP**, **DTPBT-FTP** and **DTPBT-TP**, respectively. The band gaps for all synthesized polymers in the range from 1.85 eV to 1.87 eV for polymers, **DTPBT-BTP**, **DTPBT-FTP** and **DTPBT-TP**, respectively.

The central **DTPBT** unit with the terminal isoindigo unit enhances the conjugation in the polymer. The intense ICT band in the UV-visible spectra indicates the highly conjugated nature of the polymers. The details about the photophysical properties of the synthesized polymers are summarized in Table 3.1.

In summary, the polymers exhibit interesting absorption properties, including π-π* transitions and intramolecular charge transfer, indicating their potential application in various optoelectronic devices. The presence of the **DTPBT** unit and the conjugated nature of the polymers further enhance their utility in electronic applications.

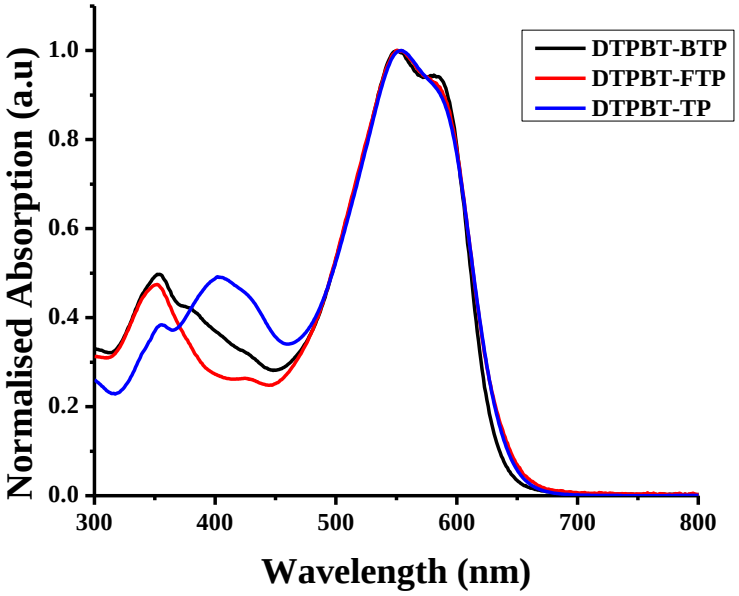

Figure 3.10 Absorption spectra of **DTPBT**-isoindigo based conjugated polymers, **DTPBT-BTP** (black line), **DTPBT-FTP** (red line) and **DTPBT-TP** (blue line).

Table 3.1 Photophysical properties of compound **DTPBT-IIG** and Photophysical properties, Thermogravimetric analysis (TGA) and Gel Permeation Chromatography analysis (GPC) of polymers, **DTPBT-BTP**, **DTPBT-FTP** and **DTPBT-TP.**

Compound	λ_{max} (nm)	λ_{edge} (nm)	E_g^{opt} (eV)[a]	T_d (°C)	M_w (Dalton)	PDI (Đ)
DTPBT-IIG	351,580	629	1.97	--	--	--
DTPBT-BTP	353, 583	661	1.87	350	14572	1.35
DTPBT-FTP	348, 553	667	1.85	294	13039	1.88
DTPBT-TP	403, 555	666	1.86	353	12888	1.66

Decomposition temperature T_d (obtained from TGA), Molecular weight M_w and poly-dispersity index (Đ, obtained from GPC analysis) of conjugated polymers, **DTPBT-BTP**, **DTPBT-FTP** and **DTPBT-TP**; [a]calculated using equation $E_g^{opt} = 1240/\lambda_{edge}$.

Electrochemical properties of monomer

The frontier orbital energy level diagram for **DTPBT-IIG** was measured by cyclic voltammetry (CV) analysis. The CV measurements were performed in a dry acetonitrile-chloroform (7:3) solution using tetra-*n*-butylammonium hexafluorophosphate ($TBAPF_6$) as a supporting electrolyte (~50 mM). The three-

electrode system consists of a Pt disc electrode as the working electrode, a Pt wire electrode as the counter electrode and Ag/Ag^+ reference electrode was used for CV measurement. Compound **DTPBT-IIG** was dissolved in dry acetonitrile (~5 mM), degassed with nitrogen gas and subjected to the CV measurements.

The π-extended conjugated **DTPBT-IIG** showed irreversible oxidation potential as shown in Figure 3.11. The oxidation potential of **DTPBT-IIG** was found at +0.95 V with onset oxidation potential at +0.80 V. The HOMO (highest occupied molecular orbital) energy levels were calculated from the onset oxidation potential which found to be at -5.55 eV The corresponding HOMO energy level was calculated from the onset oxidation potentials and found to be at −5.17 eV. The lowest unoccupied molecular orbital (LUMO) energy level was calculated by using the equation: $E_{LUMO} = E_{HOMO} + E_g^{opt}$ and was found to be at -3.58 eV.

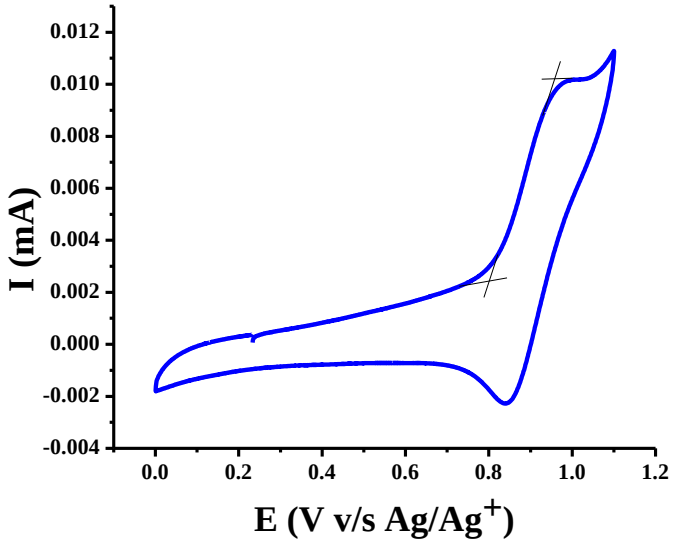

Figure 3.11 Oxidation curves of compound **DTPBT-IIG** obtained by cyclic voltammetry at 50 mV/s in dry acetonitrile-chloroform (7:3) system using $TBAPF_6$ as supporting electrolyte; $\boldsymbol{E_{onset\ Fc/Fc^+} = 0.50\ V}$

Electrochemical properties of polymers

Cyclic voltammetry (CV) analysis was used to measure the frontier orbital energy level diagram for DTPBT-isoindigo based π-extended conjugated polymers, **DTPBT-BTP**, **DTPBT-FTP** and **DTPBT-TP**. In a dry acetonitrile-chloroform (7:3) solution, tetra-*n*-butylammonium hexafluorophosphate ($TBAPF_6$) was used as a supporting electrolyte (~50 mM) for the CV measurements. The Ag/Ag^+ reference

electrode was utilised for CV measurement, and the Pt disc electrode served as the working electrode and the Pt wire electrode as the counter electrode in the three-electrode setup. After dissolving the polymers, **DTPBT-BTP**, **DTPBT-FTP** and **DTPBT-TP** in dry acetonitrile (5 mM), nitrogen gas was used to degas the mixture and the CV measurements were performed.

All the synthesized polymers showed irreversible oxidation curve in the cyclic voltammetry (CV) (Figure 3.12). The oxidation potential of polymers, **DTPBT-BTP** and **DTPBT-TP** were found to be at +0.79 V and +0.65 V, respectively. The oxidation potential of polymer **DTPBT-FTP** was not resolved. The obtained onset oxidation potentials of polymers, **DTPBT-BTP**, **DTPBT-FTP** and **DTPBT-TP** were found to be at +0.57 V, +0.56 V and +0.84 V, respectively. The HOMO energy levels of the polymers, **DTPBT-BTP**, **DTPBT-FTP** and **DTPBT-TP** were calculated from the onset oxidation potential and found to be at -5.32 eV, -5.31 eV and -5.59 eV, respectively. The LUMO energy levels were calculated by using the equation: $\boldsymbol{E_{LUMO} = E_{HOMO} + E_g^{opt}}$ and the values were found to be at 3.45 eV, 3.46 eV and 3.73 eV for the polymers, **DTPBT-BTP**, **DTPBT-FTP** and **DTPBT-TP**, respectively**.** The electrochemical properties of compound **DTPBT-IIG** and polymers were summarised in Table 3.2.

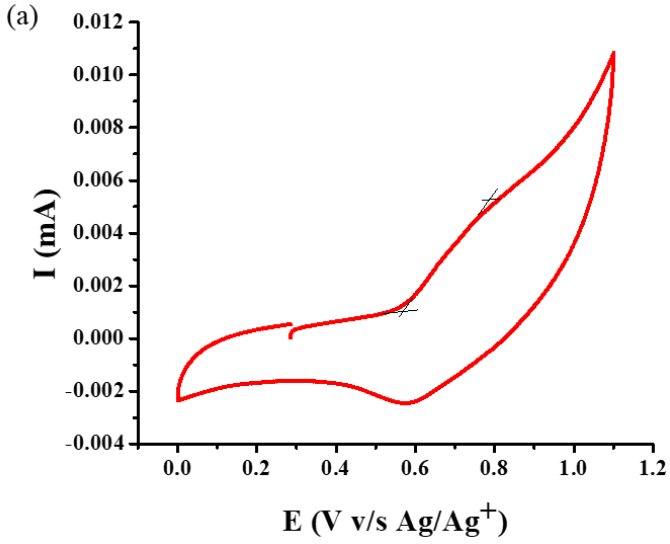

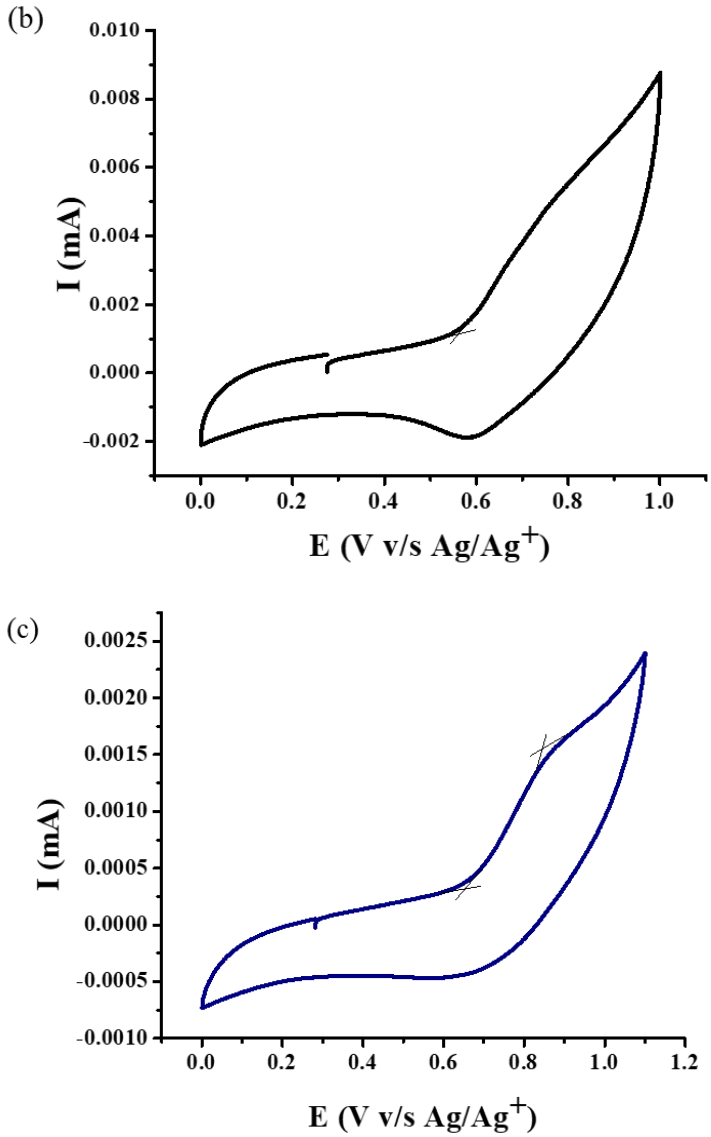

Figure 3.12 Oxidation curves of (a) polymer **DTPBT-BTP** (c) polymer **DTPBT-FTP** and (d) polymer **DTPBT-TP,** obtained by cyclic voltammetry at 50 mV/s in dry acetonitrile-chloroform (7:3) system using $TBAPF_6$ as supporting electrolyte; $\boldsymbol{E_{onset\ Fc/Fc^+} = 0.50\ V}$

Table 3.2 Electrochemical properties of compound **DTPBT-IIG** and π-extended DTPBT-isoindigo based conjugated polymers, **DTPBT-BTP**, **DTPBT-FTP** and **DTPBT-TP**

Compound/ Polymer	E_{oxi} (V) [a]	$E_{onset\ oxi}$ (V) [a]	E_{HOMO} (eV) [b]	E_{LUMO} (eV) [c]
DTPBT-IIG	+0.95	+0.80	−5.55	−3.58
BTPBT-BTP	+0.79	+0.57	−5.32	−3.45
DTPBT-FTP	-[d]	+0.56	−5.31	−3.46
DTPBT-TP	+0.65	+0.84	−5.59	−3.73

[a]Potential *v/s* Ag/Ag^+; [b]calculated from equation $E_{HOMO} = -(E_{onset\ oxi} + 4.8 - E_{onset\ Fc/Fc^+})$; [c]calculated from equation $E_{LUMO} = E_{HOMO} + E_g^{opt}$; [d]unresolved peak.

Computational studies

The density functional theory (DFT) calculation of compound **DTPBT-IIG** was performed at the B3LYP/6-31G(d) level using model compound (by substituting *N*-alkyl with *N*-ethyl groups) in order to examine the structural and electronic properties (Figure 3.13). [33,56]

The calculated HOMO-LUMO gap of **DTPBT-IIG** was found to be 2.4 eV. Model polymers, **DTPBT-BTP**, **DTPBT-FTP** and **DTPBT-TP** were optimized at B3LYP/6-31G(*d*) level.[33,56,57]The optimized structures of polymers showed that all polymers were linear. The band gap values of model polymers, **DTPBT-BTP**, **DTPBT-FTP** and **DTPBT-TP** were found to be at 2.33 eV, 2.34 eV and 2.33 eV, respectively (Figure 3.14). Table 3.3 showed the HOMO and LUMO of polymers, **DTPBT-BTP**, **DTPBT-FTP** and **DTPBT-TP**. HOMO was delocalized over whole molecules whereas LUMO was concentrated on the π-extended isoindigo parts.

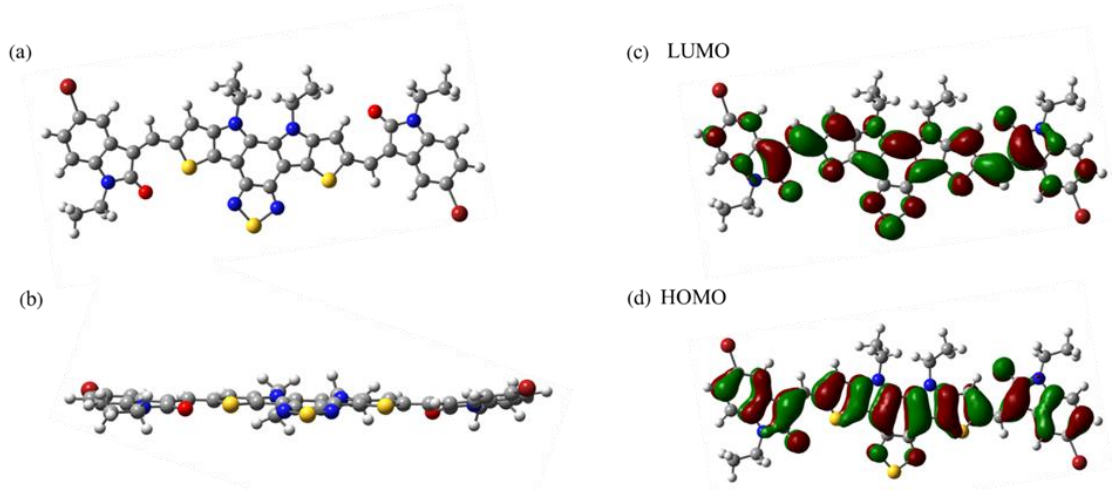

Figure 3.13 DFT calculated (a, b) optimised structure of compound **DTPBT-IIG** (c, d) HOMO-LUMO energy level diagram of compound **DTPBT-IIG**

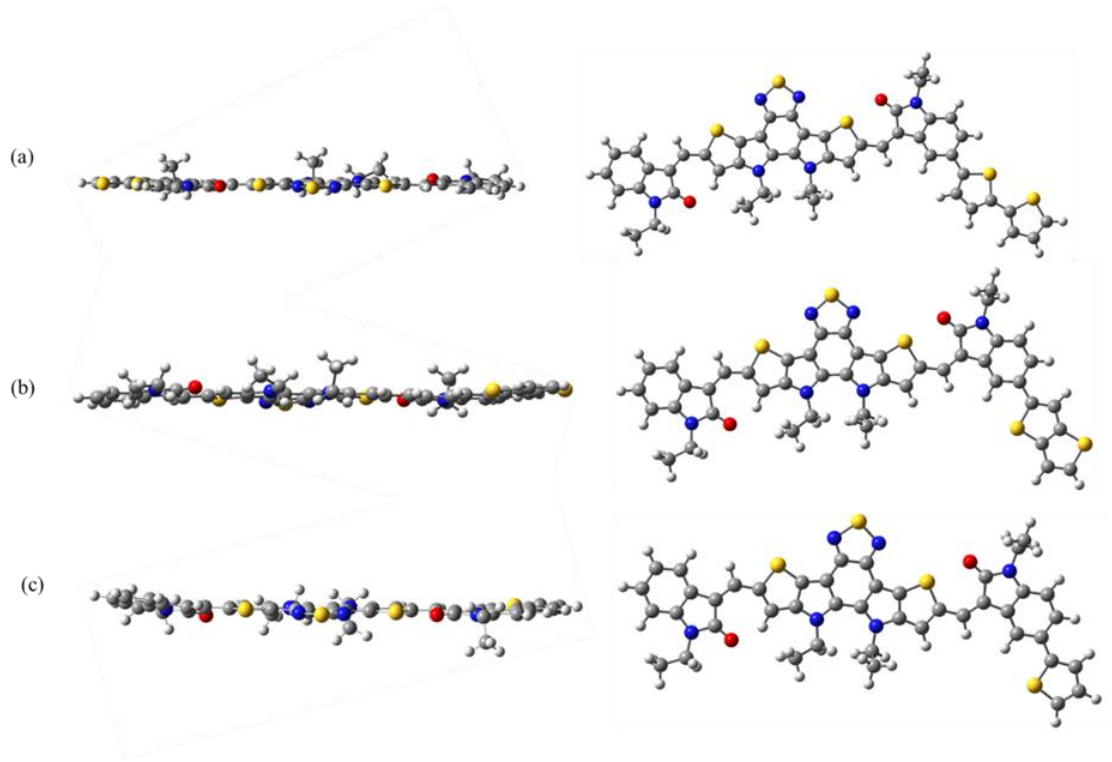

Figure 3.14 Optimised structures (a) Polymer **DTPBT-BTP**, (b) Polymer **DTPBT-FTP** and (c) Polymer **DTPBT-TP.**

Table 3.3 DFT (B3LYP/6-31G(*d*)) calculated structures, HOMO-LUMO of polymers, **DTPBT-BTP**, **DTPBT-FTP** and **DTPBT-TP**

polymer	HOMO	LUMO	Band gap
DTPBT-BTP	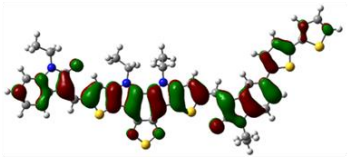	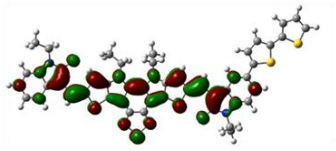	2.33
DTPBT-FTP	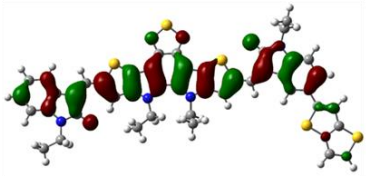	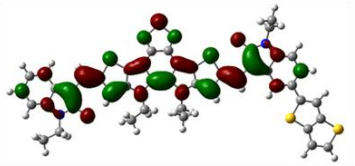	2.34
DTPBT-TP	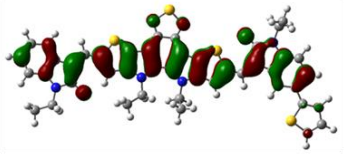	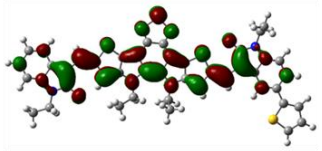	2.33

Device fabrication and characterization

By using space-charge limited current (SCLC) method, hole transporting ability of a hole transporting materials (HTMs) was being determined. For the fabrication of device firstly the ITO substrate cleaned with SDS solution, followed by triple distilled water and then acetone, kept in the sonication bath for 20 minutes. Undesired area of the ITO substrate was being converted into non-conductive part by chemical etching. One electrode was prepared by spin coating commercial PEDOT:PSS with ethanol as solution in the ratio of 1:2 ($V_{colloidal\ dispersion}$:$V_{ethanol}$) at 1500 rpm for 60 seconds on ITO substrate, which was further annealed on a hotplate for 10 minutes at 110 °C. Another electrode was prepared by spin coating HTM which was dissolved in chloroform at 1,000 rpm, three times for 60 seconds on Al foil attached to a glass substrate. The electrodes were sandwiched together as anode and cathode with configuration of ITO/PEDOT:PSS/HTM/Al.

By using a CHI660E (CHI instrument, Inc. Austin TX) at 100 mV s^{-1}, Current density-voltage characterizations were performed. DTPBT-based polymer's current density was measured by fitting *Log J v/s Log V* curves and hole carrier mobility was calculated by using the Mott– Gurney equation, [33,37,58]

$$J = \frac{9}{8}\varepsilon_0\varepsilon_r\mu\frac{V^2}{L^3}$$

where, J = current density, ε_o = vacuum permittivity (8.85×10^{-12} Fm^{-1}), ε_r = dielectric constant of the material (generally for organic semiconductors=3), μ = hole mobility, L= film thickness, and V = applied voltage.

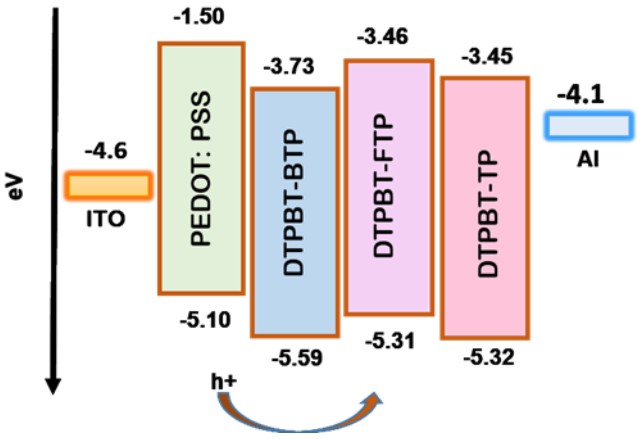

Figure 3.15 The energy level diagram of polymers.

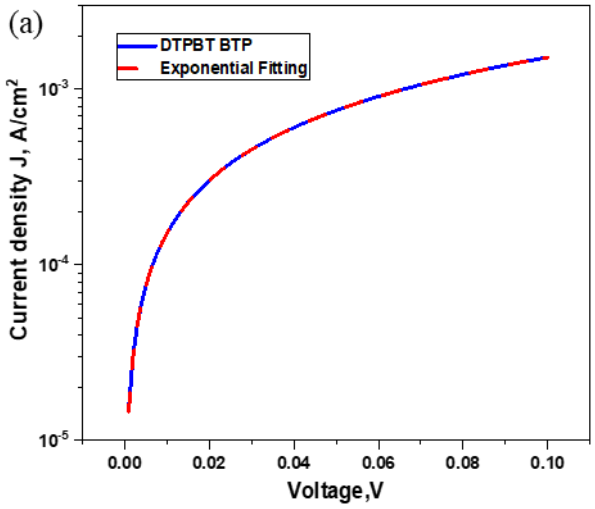

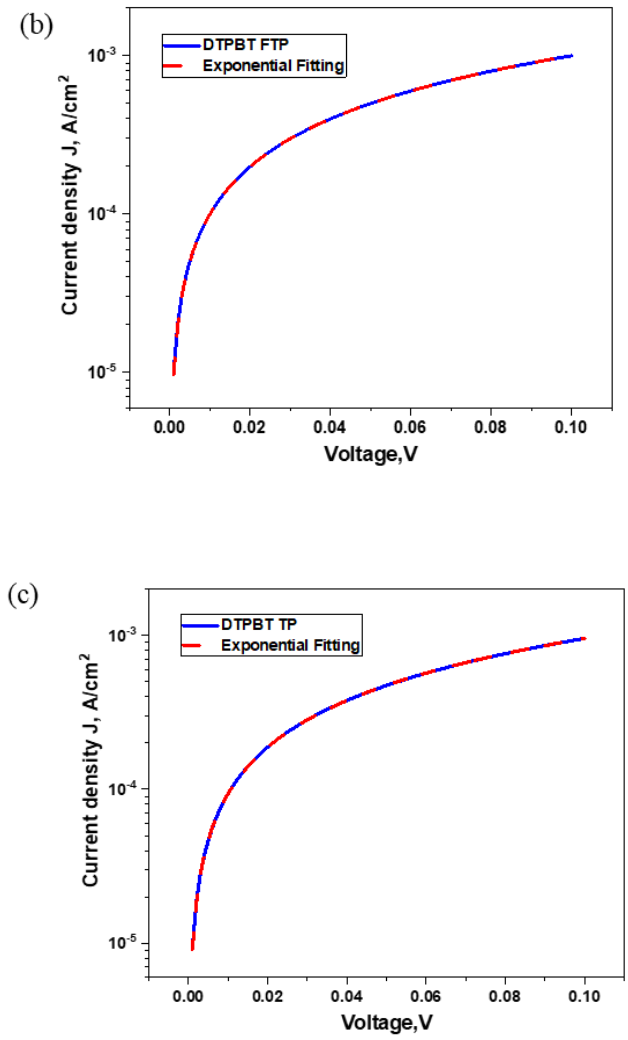

Figure 3.16 SCLC hole mobilities of polymers, (a) **DTPBT-BTP** (b) **DTPBT-FTP** and (c) **DTPBT-TP.**

Table 3.4 SCLC hole mobilities of polymers

HTMs	Hole mobility μ, $cm^2 V^{-1} s^{-1}$
DTPBT-BTP	$1.02 \pm 0.47 \times 10^{-1}$
DTPBT-FTP	$1.17 \pm 0.47 \times 10^{-1}$
DTPBT-TP	$2.51 \pm 0.47 \times 10^{-2}$

Performance of a hole only device using **DTPBT**-isoindigo based conjugated polymer was exceptionally good as it has large π-conjugated structure that builds up π-π intermolecular interaction results in better intermolecular charge transfer. It has donor and acceptor moieties with ladder structure provides planarized form with impressive

conjugation.[33,37] Here, as we change the side chain moieties, difference in charge transfer occurs. In polymer **DTPBT-TP** structure, side chain is single thiophene moiety which has lower electron density (higher *p*-type character) as compared to polymers, **DTPBT-BTP** and **DTPBT-FTP**. Thus, polymer **DTPBT-TP** exhibited higher hole mobility over other two polymers.[19,58]

Conclusion

A novel **DTPBT**-isoindigo-based conjugated building block was synthesized using a double Knoevenagel condensation reaction. Density Functional Theory (DFT) study revealed that **DTPBT**-isoindigo is nearly planar. The other unit of the comonomer (thiophene/bithiophene/thienothiophene) deviated from the DTPBT-isoindigo unit by approximately 25-30°. Optical band gap values of polymers, **DTPBT-BTP, DTPBT-FTP** and **DTPBT-TP** were determined to be 1.95 eV, 1.91 eV, and 1.93 eV, respectively. Gel Permeation Chromatography (GPC) analysis revealed that the chain length of polymers comprised 12, 10, and 10 comonomer units for polymers, **DTPBT-BTP, DTPBT-FTP** and **DTPBT-TP**, respectively. Thermogravimetric analysis (TGA) of polymers indicated considerable stability up to 290 °C. HOMO energy levels were found to be below -5.0 eV for all polymers. LUMO energy levels of polymers were in the range of -3.5 eV to -3.3 eV. Space-Charge Limited Current (SCLC) hole mobilities of polymers, **DTPBT-BTP, DTPBT-FTP** and **DTPBT-TP** were found to be $1.02 \pm 0.47 \times 10^{-1}$ cm^2 V^{-1} s^{-1}, $1.17 \pm 0.47 \times 10^{-1}$ cm^2 V^{-1} s^{-1} and $2.51 \pm 0.47 \times 10^{-2}$ cm^2 V^{-1} s^{-1}, respectively. The excellent performance of hole-only devices for all polymers was attributed to the extensive π-conjugated structure fostering π-π* intermolecular interaction and enhancing intermolecular charge transfer. Based on the preliminary data, the newly synthesized conjugated polymers (**DTPBT-BTP, DTPBT-FTP** and **DTPBT-TP**) show promise as potential candidates for various organic electronic devices.

Overall, the study provides a comprehensive analysis of the newly synthesized conjugated polymers, highlighting their structural, optical, thermal, and electronic properties, and suggests their potential applications in organic electronic devices.

Experimental procedures

General procedure

All the chemicals are reagent grade chemicals are used without any further purification steps. Moisture-sensitive reactions are carried out in an environment of dry nitrogen, which helps to exclude moisture. The solvents used in these reactions are also dried. All the reactions are monitored by thin-layer chromatography (TLC) Merck 60 F254 aluminium-coated plates are used for TLC analysis. TLC plates allow for the separation and visualization of different compounds in a mixture. The spots on the plates are visualized under ultraviolet (UV) light. Purification of all the compounds was done by column chromatography in which silica gel is used as the stationary phase for column chromatography. Two different mesh sizes, 60–120 mesh and 100–200 mesh, used for different applications. NMR spectra are recorded using a Bruker Avance-III 400 spectrometer with two different solvents $CDCl_3$ and DMSO-D^6. High resolution mass spectra are recorded using an Xevo G2-XS QTOF Mass Spectrometer. Mass spectrometry is a technique used to determine the molecular mass and structural information of compounds. Molecular weights of polymer samples are measured using an Agilent 1260 Infinity GPC instrument equipped with a refractive index (RI) detector. Polystyrene is used as a calibration standard. GPC is a technique used to determine the molecular weight distribution of polymers.

Synthesis of 5-bromo-1-(2-ethylhexyl)indolin-2-one

Compound **1** is synthesized according to the modified literature procedure reported by Li *et al.* [50,51] while compound **2** is synthesized according to the modified literature procedure reported by Bura *et al*.[52]

Synthesis of 5-bromo-1-(2-ethylhexyl) indoline-2,3-dione (1): 5-Bromoisatin (2.26 g, 10.00 mmol) and K_2CO_3 (6.20 g, 45.00 mmol) are added to the 20 mL anhydrous DMF under nitrogen atmosphere and are stirred at 60 ^oC for 5 min. To this stirred solution, 2-ethylhexylbromide (4.25 mL, 17.50 mmol) is added drop-wise and the temperature is increased to 80 ^oC. The reaction mixture is allowed to stir for 2 h, after which the reaction mixture is poured into 200 mL of water and extracted with ethyl acetate. Combined organic phase is washed with water, brine and evaporated to dryness under reduced pressure. The residual oily substance is subjected to column

chromatography over silica gel and pure product is eluted using 10% ethyl acetate-petroleum ether mobile phase.

5-Bromo-1-(2-ethylhexyl) indoline-2,3-dione (1): Red solid (3.23 g, 82%); ^{1}H NMR (400 MHz, $CDCl_3$) δ: 7.72 (d, J_3 = 1.2 Hz, 1H), 7.70 (d, J_2 = 7.6 Hz, 1H), 6.82 (dd, J_2 = 7.6 Hz, J_3 = 1.2 Hz, 1H), 3.70−3.74 (t, J_2 = 7.2 Hz, 2H), 1.65−1.73 (m, 2H), 1.26−1.34 (m, 18H), 0.87−0.91 (t, J_2 = 7.2 Hz, 3H).

Synthesis of 5-bromo-1-(2-ethylhexyl) indolin-2-one (2): Compound **1** (1.01 g, 3.77 mmol) and hydrazine hydrate, 99% (9.2 mL, 188.5 mmol) are taken in single neck round bottom flask and heated at 140 ^{o}C for 2 h under nitrogen atmosphere. After completion of the reaction, reaction mixture is dissolved in ethyl acetate, washed with water (3 X 30 mL) and dried over anhydrous sodium sulphate and concentrated under reduced pressure. To the resulting crude, 20 mL of 6 N aqueous hydrochloric acid solution is added and the resulting mixture is heated at 60 ^{o}C overnight. The reaction mixture is poured into 200 mL of water and extracted with ethyl acetate. Combined organic phase is washed with water, brine, dried over anhydrous sodium sulphate and evaporated under reduced pressure. The crude product thus obtained, is subjected to the column chromatography over silica gel. The pure product is eluted using dichloromethane as mobile phase.

5-Bromo-1-(2-ethylhexyl) indolin-2-one (2): Yellowish solid (0.82 g, 86%); ^{1}H NMR (400 MHz, $CDCl_3$) δ: 7.34−7.37 (m, 2H), 6.67−6.69 (d, J_2 = 8.0 Hz, 1H), 3.61−3.65 (t, J_2 = 7.6 Hz, 2H), 3.50 (s, 2H), 1.63−1.69 (m, 2H), 0.92−0.96 (t, J_2 = 7.6 Hz, 3H).

Synthesis of 10,11-bis(2-ethylhexyl)-10,11-dihydro-[*1,2,5*]thiadiazolo[*3,4-e*]thieno[*2',3':4,5*]pyrrolo[*3,2-g*]thieno[*3,2-b*]indole-2,8-dicarbaldehyde

Synthesis of benzo[*c*][*1,2,5*]thiadiazole (3): To a 1000 mL round bottom flask, 1,2-phenylenediamine (10.00 g, 92.47 mmol), 300 mL of dichloromethane and triethylamine (37.44 g, 369.98 mmol) are added. The solution is stirred until total dissolution of the 1,2-phenylenediamine. To this stirred reaction mixture, a solution of $SOCl_2$ in small amount of dichloromethane is added very slowly and the resulting reaction mixture is refluxed for 4 h. The solvent is removed in a rotary evaporator and resulting concentrate is diluted with 700 mL of water. The final pH of the solution is adjusted to 2 by adding concentrated HCl. The desired compound is purified by direct

steam distillation following the addition of water to the mixture. The steam distilled mixture is extracted with 3 X 200 mL of dichloromethane, dried over MgSO4 and filtered. The solvent is removed, affording pure compound **3**.

Benzo[*c*][*1,2,5*]thiadiazole (3): White solid (5.6 g, 45%); ^{1}H NMR (400 MHz, $CDCl_3$): δ 8.00−8.05 (dd, J_2 = 6.8 Hz, J_3 = 3.2 Hz, 1H), 7.59−7.63 (dd, J_2 = 6.8 Hz, J_3 = 3.2 Hz, 1H).

Synthesis of 4,7-dibromobenzo[*c*][*1,2,5*]thiadiazole (4): To a 500 mL two-necked round bottom flask, compound **3** (10.00 g, 73.44 mmol) and 150 mL of HBr (47%) are added and the reaction mixture is allowed to stir at 60 ºC for 15 min. A solution containing Br_2 (35.21 g, 220.32 mmol) in 100 mL of HBr is added drop wise to the reaction mixture. After addition of the Br_2, the resulting reaction mixture is refluxed for 6 h during which, precipitation of orange solid is observed. The mixture is allowed to cool to room temperature and un-reacted Br_2 is quenched by addition of saturated solution of $NaHSO_3$. The mixture is filtered under vacuum and washed exhaustively with water. The solid is then washed once with cold diethylether and dried under vacuum, affording the compound **4** in 95% yield.

4,7-Dibromobenzo[*c*][*1,2,5*]thiadiazole (4): Off-white solid (20.3 g, 94%); ^{1}H NMR (400 MHz, $CDCl_3$):δ 7.75 (s, 1H).

Synthesis of 4,7-dibromo-5,6-dinitrobenzo[*c*][*1,2,5*]thiadiazole (5): Compound **5** is prepared by following the literature procedure.[11] In a 150 mL two-necked round bottom flask, fuming nitric acid (1.50 g, 23.8 mmol) is added drop wise to trifluoromethanesulfonic acid (15.00 g, 100 mmol) at 0 °C. Up on complete addition of fuming nitric acid, an insoluble nitrating mixture $2CF_3SO_3H/HNO_3$ appeared as white solids immediately. To this, compound **4** (2.50 g, 8.5 mmol) is added, portion-wise over a period of 20 min to avoid exothermicity. After addition, the reaction mixture is kept stirring at 50 °C for 8 h, during which evolution of brisk red coloured gas is noted. After completion, the mixture is poured into ice water slowly, and then sodium hydroxide solution is added to neutralize the excess acid. The precipitates are filtered and washed with water. The pure product is obtained by re-crystallization of crude product from ethanol.

4,7-Dibromo-5,6-dinitrobenzo[*c*][*1,2,5*]thiadiazole (5): Yellow beige solid (2.71 g, 83%); ^{1}H NMR (400 MHz, $CDCl_3$): No proton signals observed. ^{13}C NMR (100 MHz, $CDCl_3$): δ 151.5, 143.6, 111.3.

Synthesis of 5,6-dinitro-4,7-di(thiophen-2-yl)benzo[*c*][*1,2,5*]thiadiazole (6): Compound **6** was synthesized by following the reported procedure. [55] In a 100 mL two-necked round bottom flask, compound **5** (3.80 g, 9.90 mmol), $PdCl_2(PPh_3)_2$ (0.14 g, 0.2 mmol) and 30 mL of dried THF are degassed by purging nitrogen gas through the reaction mixture for 15 min. To the degassed reaction mixture, tri-*n*-butyl(thiophene-2-yl)stannane (8.51 g, 22.8 mmol) is added and the mixture is refluxed for 3 h under nitrogen atmosphere. After cooling the reaction mixture, an orange solid appeared which is filtered off, washed with acetonitrile and dried under vacuum to give pure product as an orange solid.

5,6-Dinitro-4,7-di(thiophen-2-yl)benzo[c][1,2,5]thiadiazole (6): Orange solid (3.05 g, 79%); ^{1}H NMR (400 MHz, $CDCl_3$): δ 7.76−7.77 (dd, J2 = 4.8 Hz, J3 = 1.2 Hz, 1H), 7.53−7.54 (dd, J2 = 4.0 Hz, J3 = 1.2 Hz, 1H), 7.25−7.27 (m, 1H).

Synthesis of 10,11-dihydro-[*1,2,5*]thiadiazolo[*3,4-e*]thieno[*2',3':4,5*]pyrrolo[*3,2-g*]thieno[*3,2-b*]indole (7): In to a 250 mL two-necked round bottom flask is charged with compound **6** (1.50 g, 3.85 mmol), PPh_3 (10.08 g, 38.5 mmol) and 192 mL of 1,2-dichlorobenzene (*o*-DCB) under nitrogen atmosphere. The reaction mixture is degassed by purging nitrogen gas through the reaction mixture for 15 min. The degassed reaction mixture is refluxed under nitrogen atmosphere for 12 h. The reaction mixture is cooled to room temperature and is subjected to the column chromatography. The 1,2-dichlorobenzene along with excessive PPh_3 is eluted using petroleum ether. The pure product is eluted using 50% ethyl acetate-petroleum ether as eluent and dried under vacuum to give bright yellow air-sensitive solid.

10,11-Dihydro-[*1,2,5*]thiadiazolo[*3,4-e*]thieno[*2',3':4,5*]pyrrolo[*3,2-g*]thieno[*3,2-b*]indole (7): Bright yellow solid (0.91 g, 73%); ^{1}H NMR (400 MHz, DMSO-D_6): δ 11.90 (s, 1H), 7.61−7.63 (d, J_2 = 5.2 Hz, 1H), 7.43−7.44 (d, J_2 = 5.2 Hz, 1H).

Synthesis of 10,11-bis(2-ethylhexyl)-10,11-dihydro-[*1,2,5*]thiadiazolo[*3,4-e*]thieno[*2',3':4,5*]pyrrolo[*3,2-g*]thieno[*3,2-b*]indole (8): To a 150 mL two necked round bottom flask, take compound **7** (0.84gm, 2.56mmol), NaOH (1.025gm,

25.64mmol) was added and the reaction mixture was allowed to stir at room temperature for 10 min. The reaction mixture was than charged with 2-ethylhexyl bromide (3.21gm, 16.60mmol) and stir at 90 °C for 12h. The reaction mixture was allowed to cool at room temperature and pour into water and the organic layer was extracted with ethyl acetate. Combined organic layer was washed with water, brine, dried over anhydrous sodium sulphate and evaporated under reduced pressure. The crude product was purified by column chromatography over silica gel and pure product was eluted using 5% ethyl acetate-petroleum ether as mobile phase.

10,11-Bis(2-ethylhexyl)-10,11-dihydro-[*1,2,5*]thiadiazolo[*3,4-e*]thieno [*2',3':4,5*] pyrrolo[*3,2-g*]thieno[*3,2-b*]indole (8): Yellow solid (0.962g, 53%); ^{1}H NMR (400 MHz, $CDCl_3$): δ 7.45-7.44 (d, 1H), 7.19-7.18 (d, 1H), 4.53-4.50 (s, 2H), 2.0-1.96 (s, 1H), 1.07-0.90 (M, 9H), 0.89-0.86 (m, 6H).

Synthesis of 10,11-bis(2-ethylhexyl)-10,11-dihydro-[*1,2,5*]thiadiazolo[*3,4-e*]thieno[*2',3':4,5*]pyrrolo[*3,2-g*]thieno[*3,2-b*]indole-2,8-dicarbaldehyde (9) : In to a 100 mL round bottom flask dimethyl formamide (DMF) (3.23g, 44.16mmol), and phosphorus oxichloride ($POCl_3$) (5.91gm, 38.56mmol) was added and allowed to stir at 0 ℃ until viscous liquid was obtained. To this solution of compound **8** (0.962g, 1.45mmol) in to 1,2-dichloroethane (22 mL) was added in drop wise manner after the addition was completed the reaction mixture was allowed to stir at 80 ℃ for 12h. After the completion of reaction, it was poured in to a saturated sodium acetate solution and allowed to stir for 30 min. After that the product was filtered and washed with water and methanol.

10,11-Bis(2-ethylhexyl)-10,11-dihydro-[*1,2,5*]thiadiazolo[*3,4-e*] thieno [*2',3':4,5*] pyrrolo [*3,2-g*]thieno[*3,2-b*]indole-2,8-dicarbaldehyde (9): Yellow solid (0.74 g, 70%); ^{1}H NMR (400 MHz, $CDCl_3$): δ 10.04 (s, 1H), 7.86 (s, 1H), 4.58-4.55 (d, 2H), 1.99 (s, 1H), 1.97 (s, 1H), 1.30 (s, 3H), 1.029 (m, 5H), 1.01 (m, 6H).

Synthesis of monomer

Synthesis of (Z)-5-bromo-3-((4-((2-((Z)-5-bromo-1-(2-ethylhexyl)-2-oxoindolin-3-ylidene) ethyl)thio)-6,7-bis(2-ethylhexyl)-6,7-dihydropyrrolo[3,2-g][1,2,5]thiadiazolo[3,4-e]thieno[3,2-b]indol-9-yl)methylene)-1-(2-ethylhexyl)indolin-2-one (DTPBT-IIG): To a 100 mL round bottom flask, compound **2** (0.35g, 0.61mmol) and 2-ethylhexylindoline-2-one (**9**) (0.5g, 1.22mmol) in acetonitrile (15 mL) and chloroform (15 mL) were added and stirred at room temperature. The reaction mixture was degassed by purging nitrogen gas. To this stirred solution piperidene (0.18g, 2.13 mmol) was added drop wise and the reaction mixture was allowed to reflux for 24h. After that, the reaction mixture was cooled to room temperature and the precipitated product was collected by filtration. Filtered product was washed with copious amount of acetonitrile and dried at room temperature. The pure product was obtained by re-crystallization from petroleum ether-chloroform solution.

(*Z*)-5-Bromo-3-((4-((2-((*Z*)-5-bromo-1-(2-ethylhexyl)-2-oxoindolin-3-ylidene) ethyl)thio)-6,7-bis(2-ethylhexyl)-6,7-dihydropyrrolo[*3,2-g*][*1,2,5*]thiadiazolo[*3,4-e*]thieno[*3,2-b*]indol-9-yl)methylene)-1-(2-ethylhexyl)indolin-2-one (DTPBT-IIG) : Purple colour solid (0.39 g, 57%). ^{1}H NMR (400 MHz, $CDCl_3$): δ 8.70 (s, 1H), 7.70 - 7.66 (d, 1H), 7.39-7.37 (d, 1H), 6.77-6.75 (s, 1H), 4.59 (d, 1H), 3.78-3.74 (d, J=16Hz, 2H), 2.05 (s, 2H), 2.03-1.42 (m, 4H), 1.41-1.33 (m, 9H), 1.27-1.02 (m, 15H), 0.98-0.71(m, 7H). ^{13}C NMR (100 MHz, $CDCl_3$): δ 166.53, 147.68, 145.15, 140.45, 139.45, 134.01, 130.65, 130.38, 129.04, 126.47, 121.38, 119.89, 114.15, 111.69, 109.55, 54.30, 44.16, 39.33, 37.82, 30.90, 29.57, 28.93, 27.93, 24.11, 23.13, 22.80, 13.88, 10.91, 10.10. MALDI-TOF (ES^+): requires 1224.434 found 1224.338. IR (KBr, cm^{-1}): 3433, 2958, 2926, 2857, 1692, 1607, 1589, 1555, 1503, 1468, 1436, 1411, 1365, 1334, 1300, 1262, 1214, 1170, 1078, 1040, 957, 900, 865, 802, 775, 728, 669, 612.

Synthesis of polymer

Polymers, **DTPBT-BTP, DTPBT-FTP** and **DTPBT-TP** were synthesized by coupling of compound **DTPBT-IIG** with 5,5'-bis(trimethylstannyl)-2,2'-bithiophene, 2,5-bis(trimethylstannyl)thieno[3,2-*b*]thiophene and 2,5-bis(trimethylstannyl)thiophene, respectively in presence of $Pd_2(dba)_3$ and tri-*o*-tolylphosphine as the catalyst-ligand

system in toluene. Detailed experimental procedure for polymerization is mentioned below.

General procedure for synthesis of DTPBT based conjugated polymers DTPBT-BTP, DTPBT-FTP and DTPBT-TP

To an oven dried two necked round bottom flask compound **DTPBT-IIG** (0.3 g, 0.30 mmol, 1 eq) and 5,5'-bis(trimethylstannyl)-2,2'bithiophene (1.05 eq) or 2,5-bis(trimethylstannyl)thieno[3,2-*b*] thiophene (1.05 eq) or 2,5-bis(trimethylstannyl)thiophene (1.05 eq) were added. To this $Pd_2(dba)_3$ (0.05 mole %), tri-*o*-tolylphosphine (0.21 mole%), 20 mL of anhydrous toluene were added under nitrogen atmosphere. The resulting solution was degassed by purging nitrogen for 20 minutes. The reaction mixture is then heated at 120 ℃ for 72h. After that 2-bromothiophene (0.1 mL) was added and reaction mixture was stirred for further 2h. After completion of reaction, the reaction mixture was allowed to cool at room temperature, toluene was evaporated under vacuum and polymer were precipitated by adding methanol. Resulting precipitate were filtered and washed with methanol. Obtained crude polymer were subjected to Soxhlet extraction using methanol, acetone, pet ether and chloroform. The polymers were obtained by evaporation of chloroform under reduced pressure and further dried under vacuum at 50 ℃to yield corresponding polymers.

Polymer DTPBT-BTP: Dark purple colour polymer obtained with 46% yield. ^{1}H NMR (400 MHz, $CDCl_3$): δ 8.72 (br s, 1H), 7.49 (br s, 3H), 7.20 (br s, 3H), 6.86 (br s, 2H), 4.63 (br s, 2H), 3.77 (br s, 2H), 1.94 (22H), 1.27 (37H).

Polymer DTPBT-FTP: Dark purple colour polymer obtained with 49% yield. ^{1}H NMR (400 MHz, $CDCl_3$): δ 8.43 (br s, 1H), 8.17 (br s, 2H), 7.58 (br s, 3H), 7.36 (br s, 2H), 6.72 (br s, 2H), 3.77 (br s, 2H), 1.69 (37H), 0.80 (br s, 5H).

Polymer DTPBT-TP: Purple coloured polymer obtained with 52% yield. ^{1}H NMR (400 MHz, $CDCl_3$): δ 8.21 (br s, 1H), 6.85 (br s, 7h), 3.76 (br s, 2H), 0.88 (br s, 32H).

Spectral data

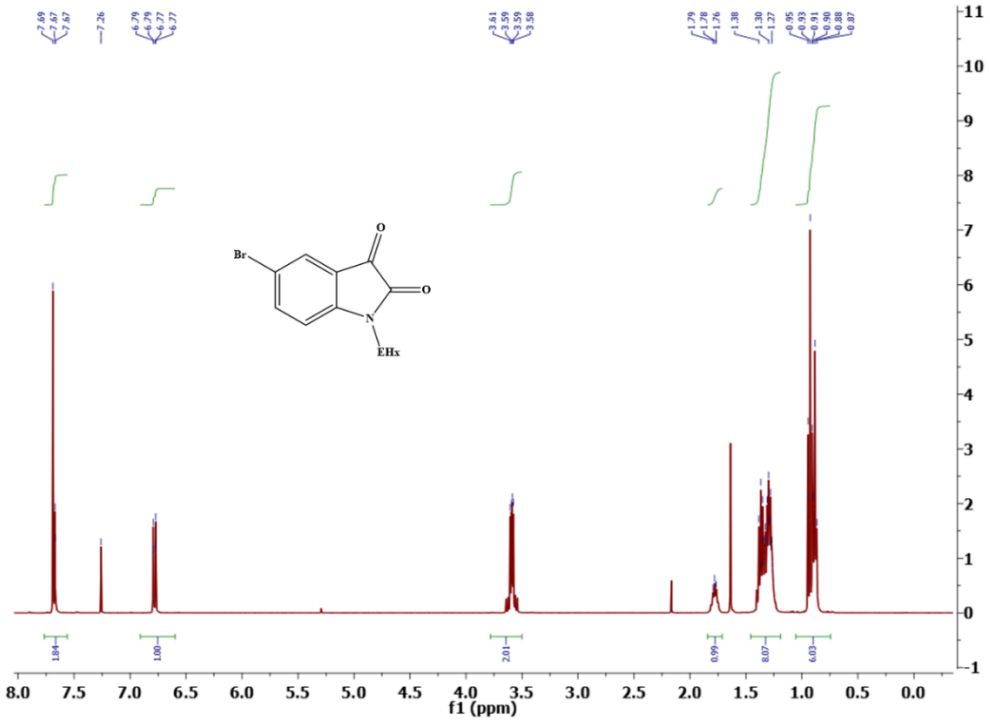

Figure 3.17 ^{1}H NMR spectra of compound **1**

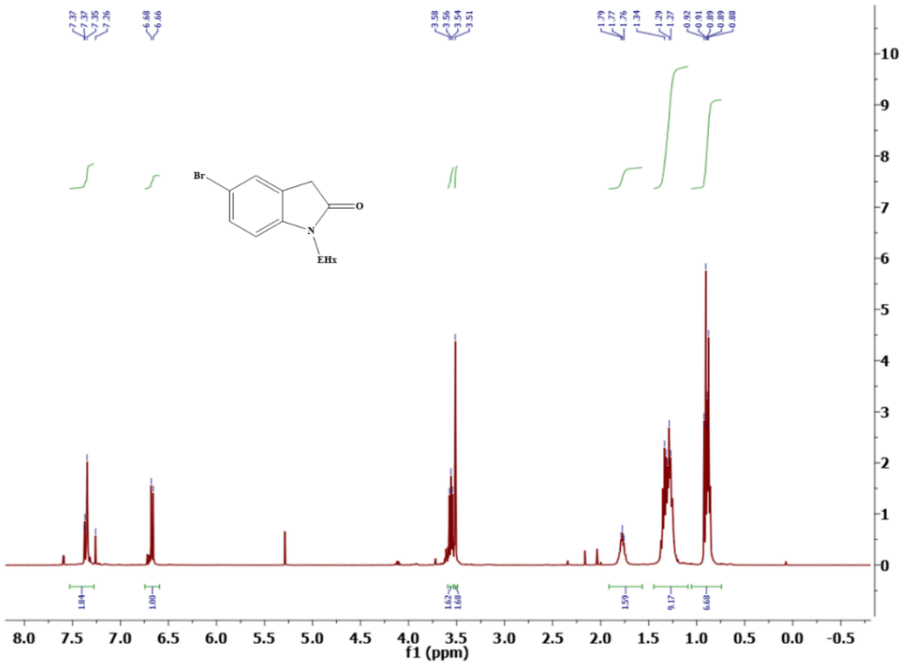

Figure 3.18 ^{1}H NMR spectra of compound **2**

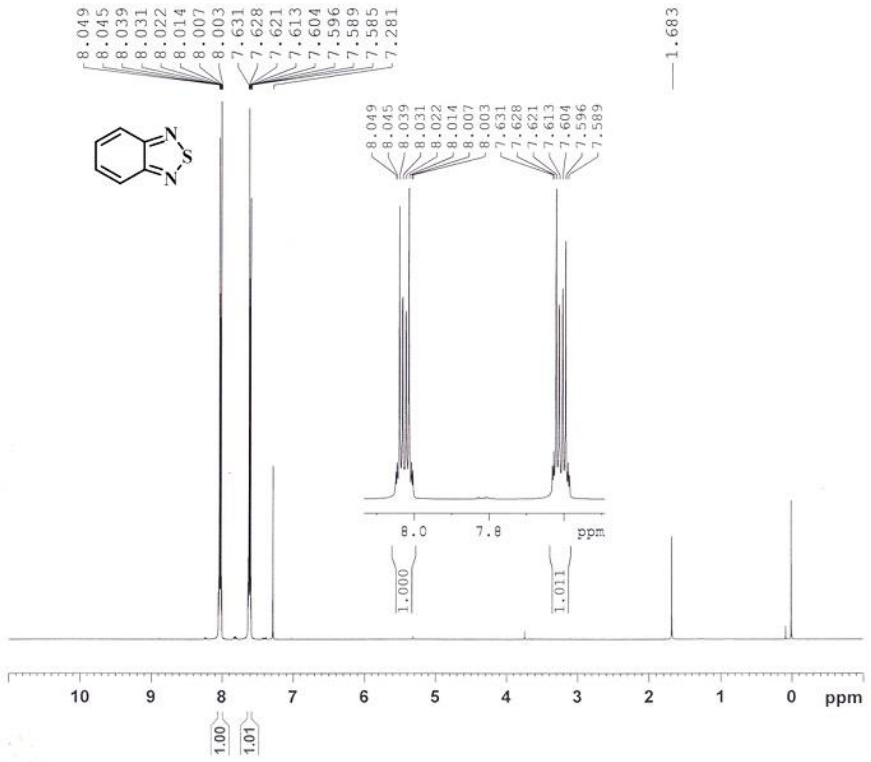

Figure 3.19 ^{1}H NMR spectra of compound **3**

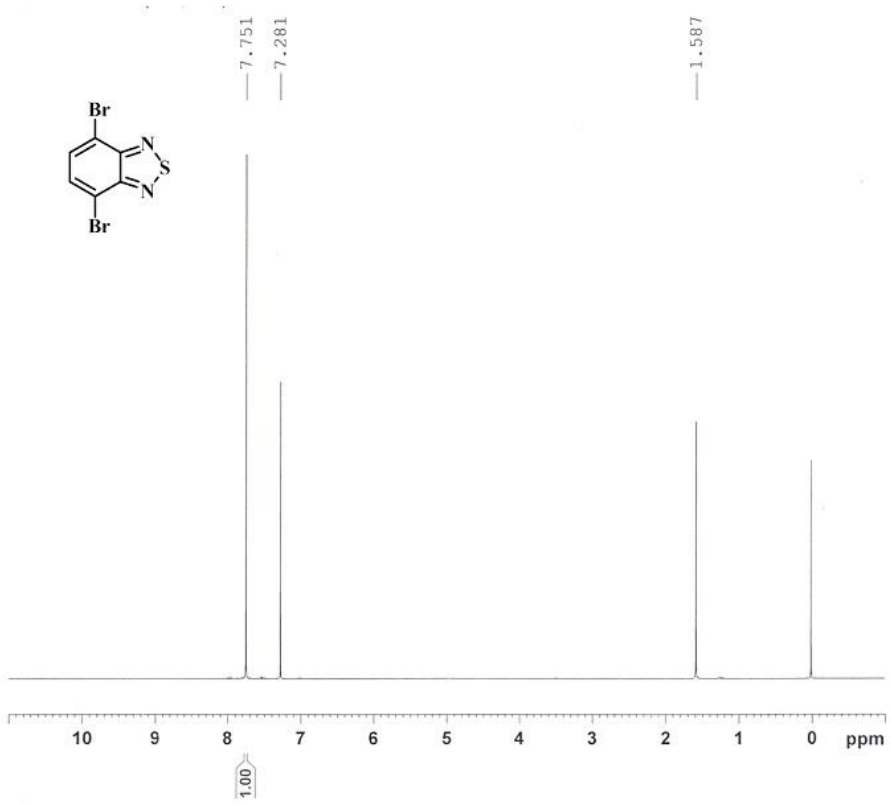

Figure 3.20 ^{1}H NMR spectra of compound **4**

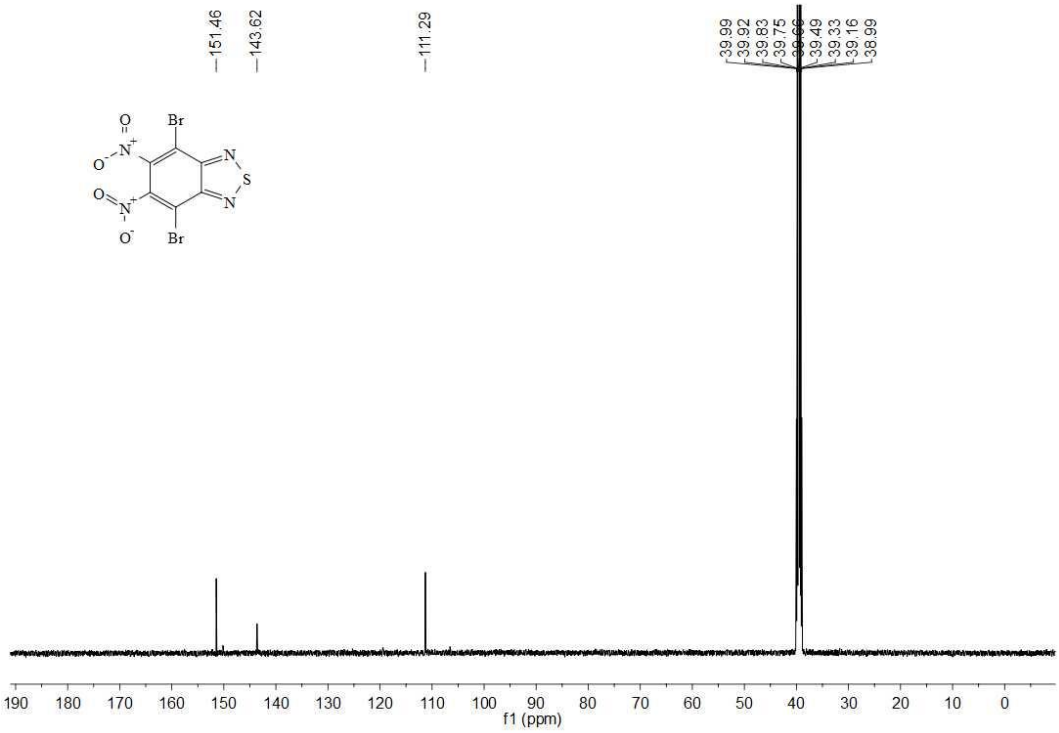

Figure 3.21 ^{13}C NMR spectra of compound **5**

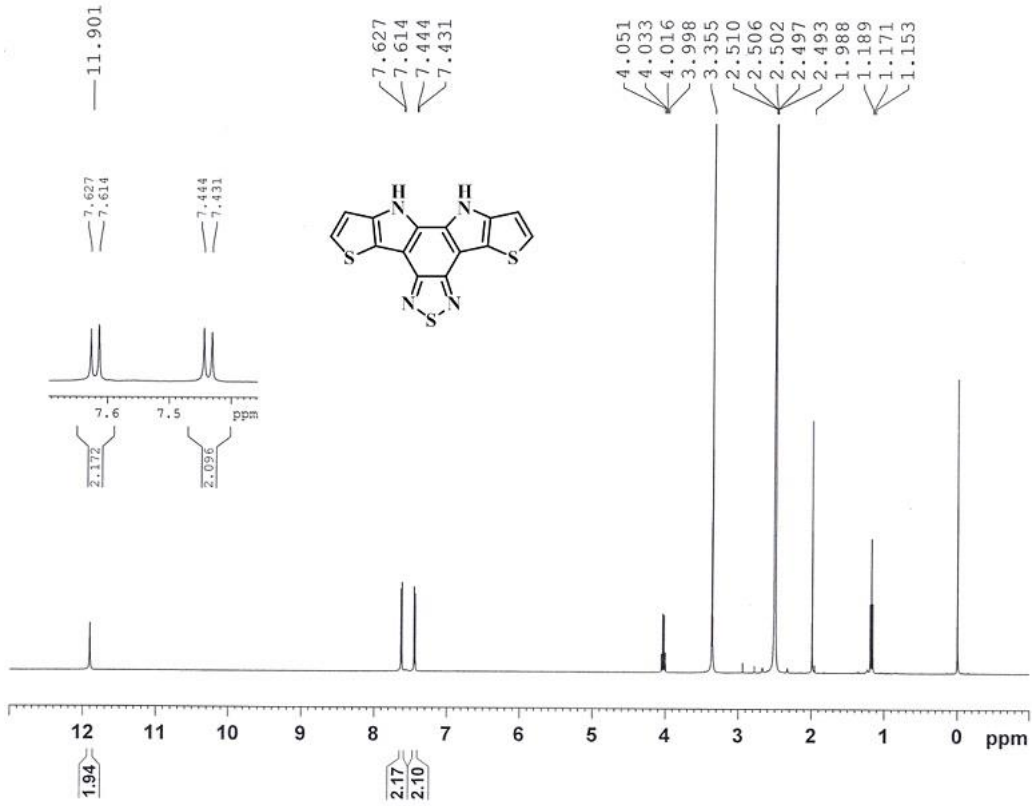

Figure 3.22 ^{1}H NMR spectra of compound **6**

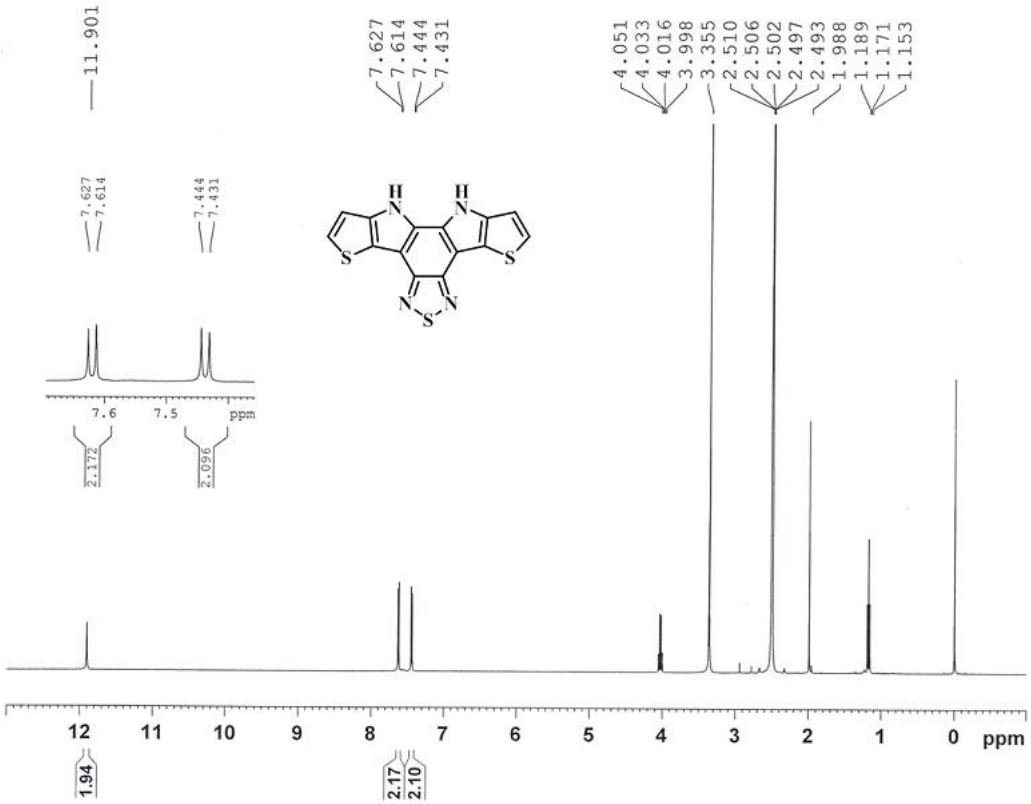

Figure 3.23 ^{1}H NMR spectra of compound **7**

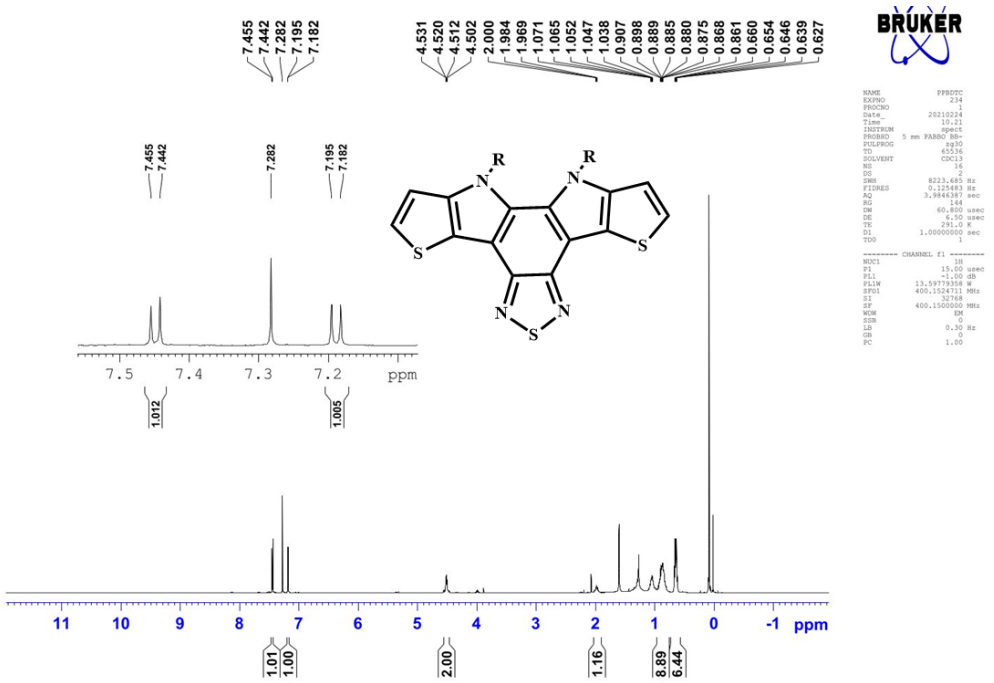

Figure 3.24 ^{1}H NMR spectra of compound **8**

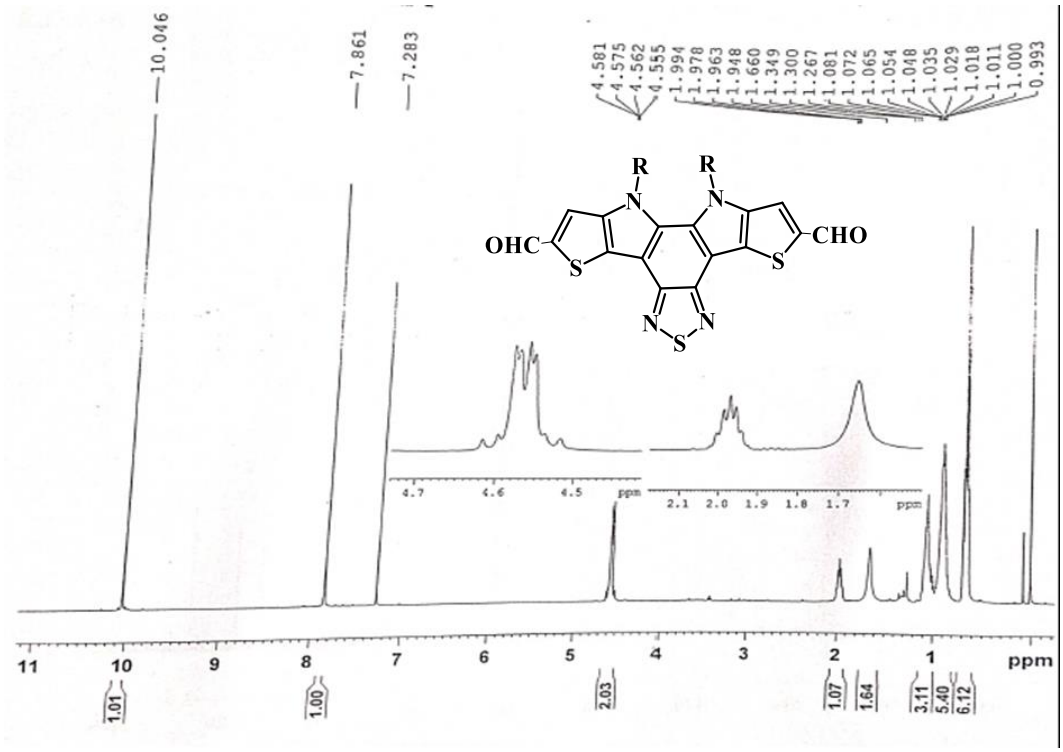

Figure 3.25 ^{1}H NMR spectra of compound **DTPBT**

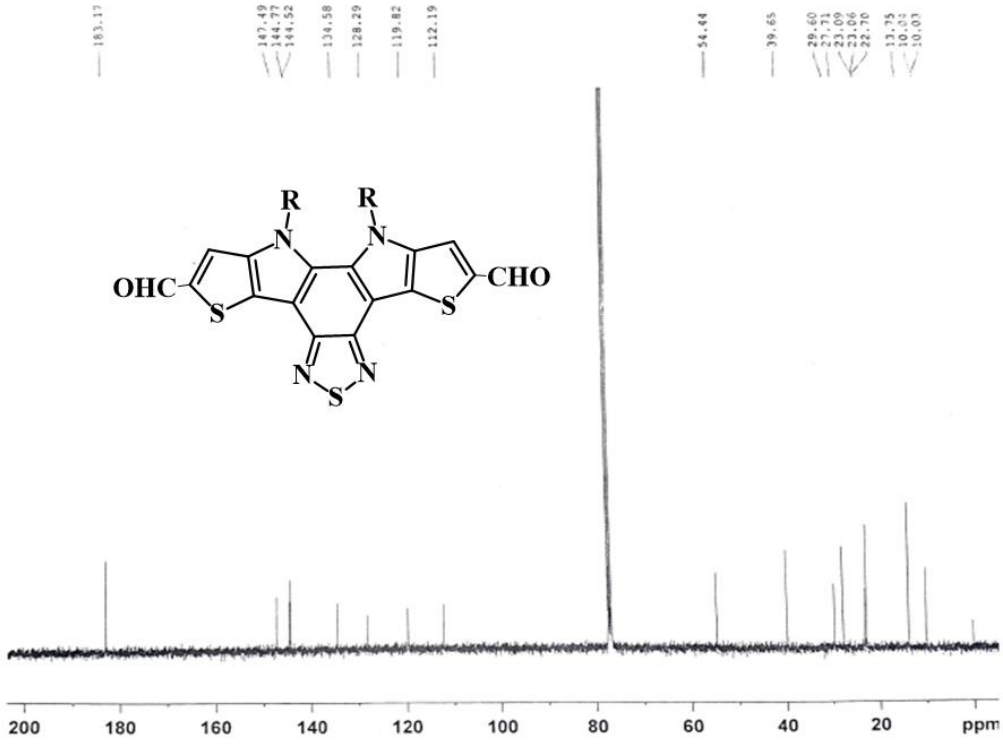

Figure 3.26 ^{13}C NMR spectra of compound **9**

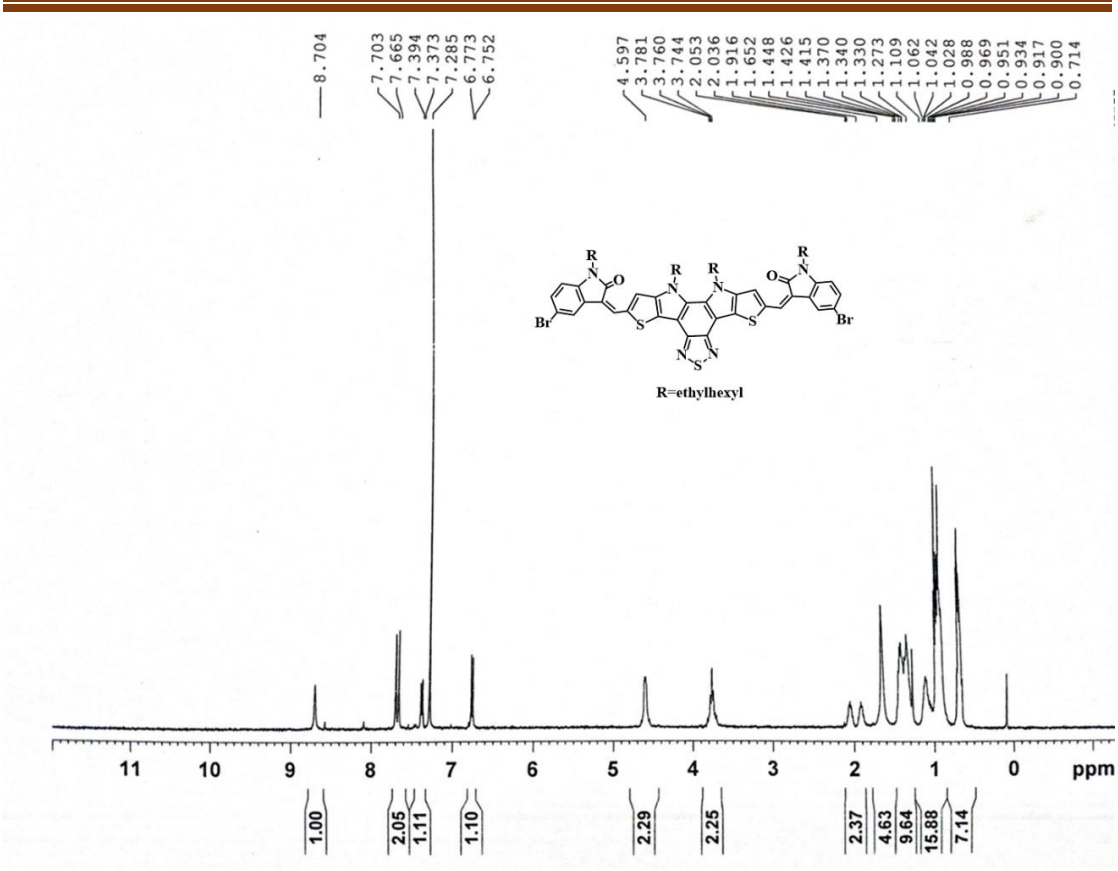

Figure 3.27 ^{1}H NMR spectra of compound **DTPBT-IIG**

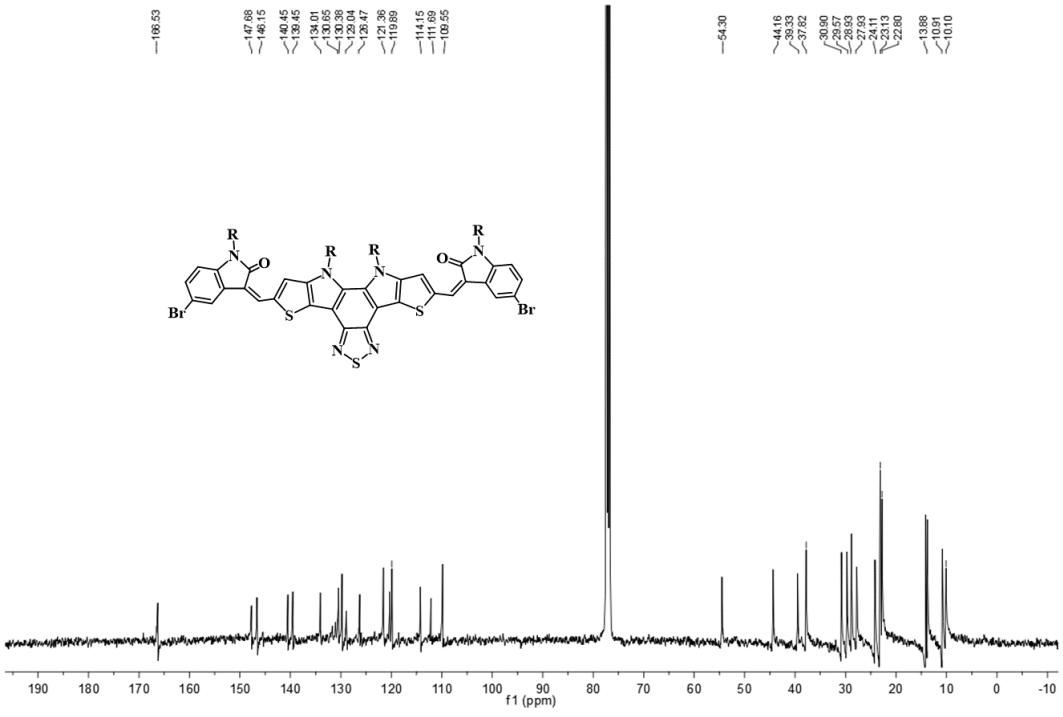

Figure 3.28 ^{13}C NMR spectra of compound **DTPBT-IIG**

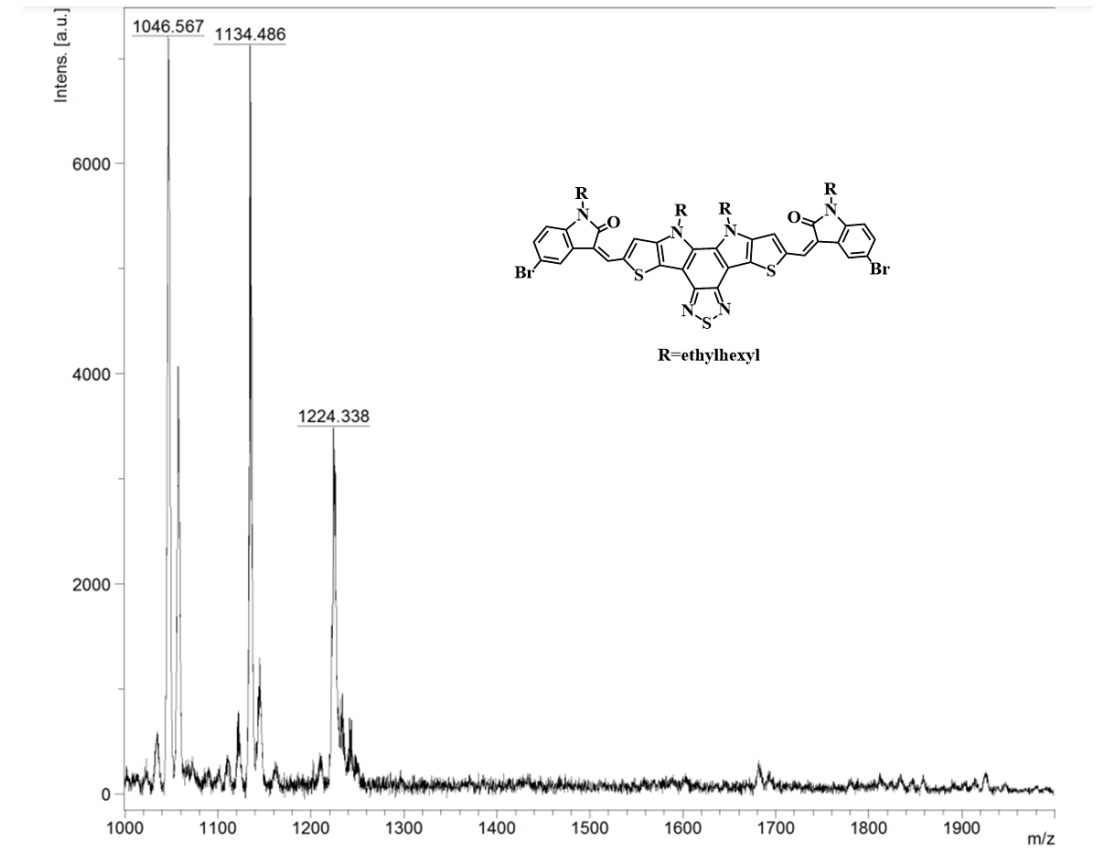

Figure 3.29 MALDI-TOF analysis of **DTPBT-IIG**

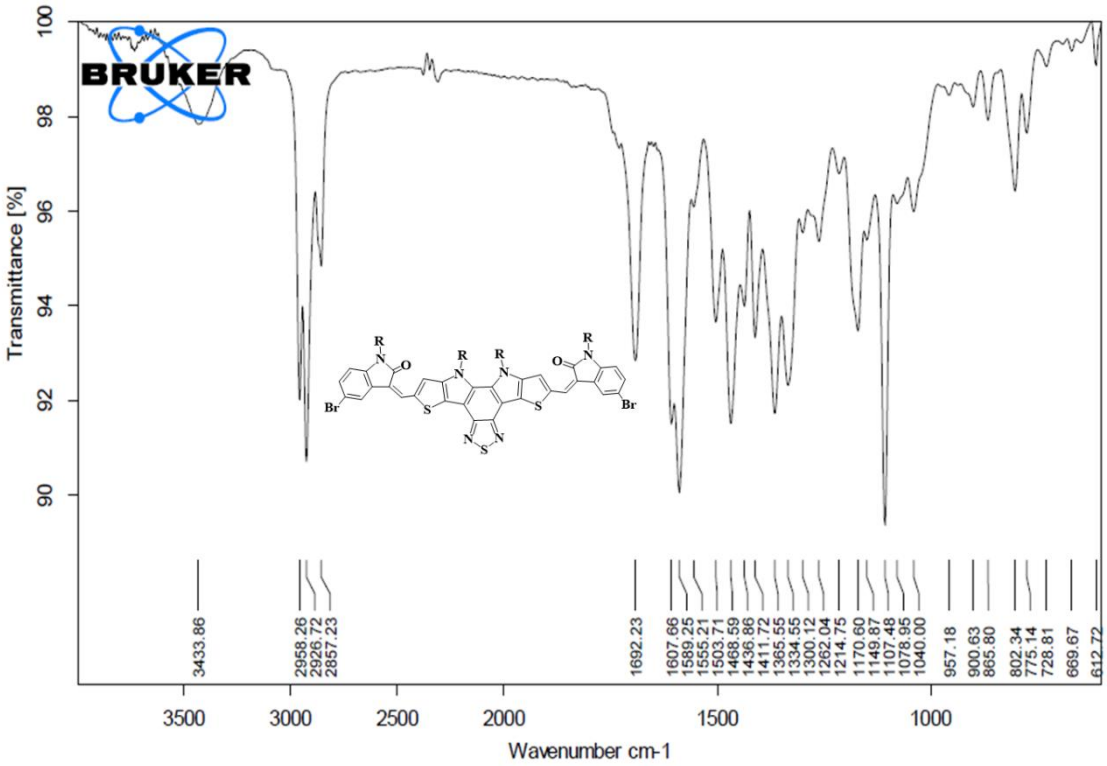

Figure 3.30 IR data of **DTPBT-IIG**

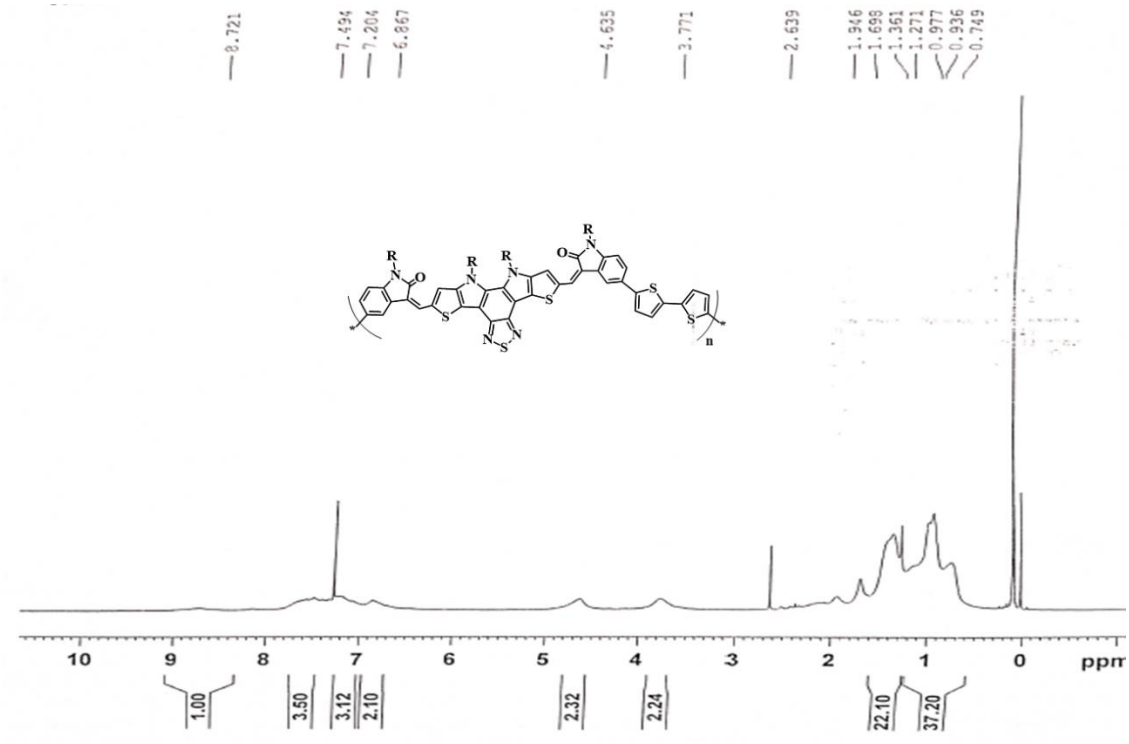

Figure 3.31 ^{1}H NMR spectrum of **DTPBT-BTP**

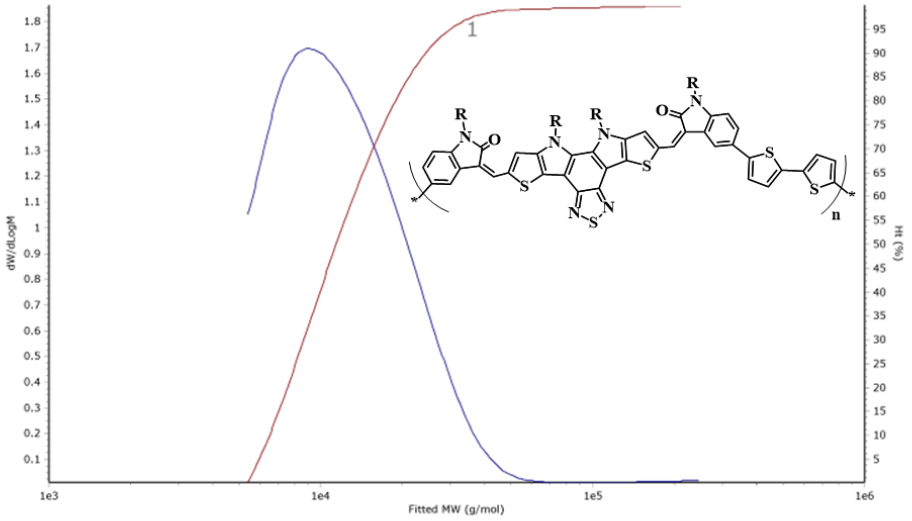

Results

Analysed by Applied Chem at 15:59:21 on 04 August 2022

Comments

Molecular Weight Averages

Peak	Mp (g/mol)	Mn (g/mol)	Mw (g/mol)	Mz (g/mol)	Mz+1 (g/mol)	Mv (g/mol)	PD
Peak 1	9261	10783	14572	28649	89416	24414	1.351

Figure 3.32 GPC data of polymer **DTPBT-BTP**

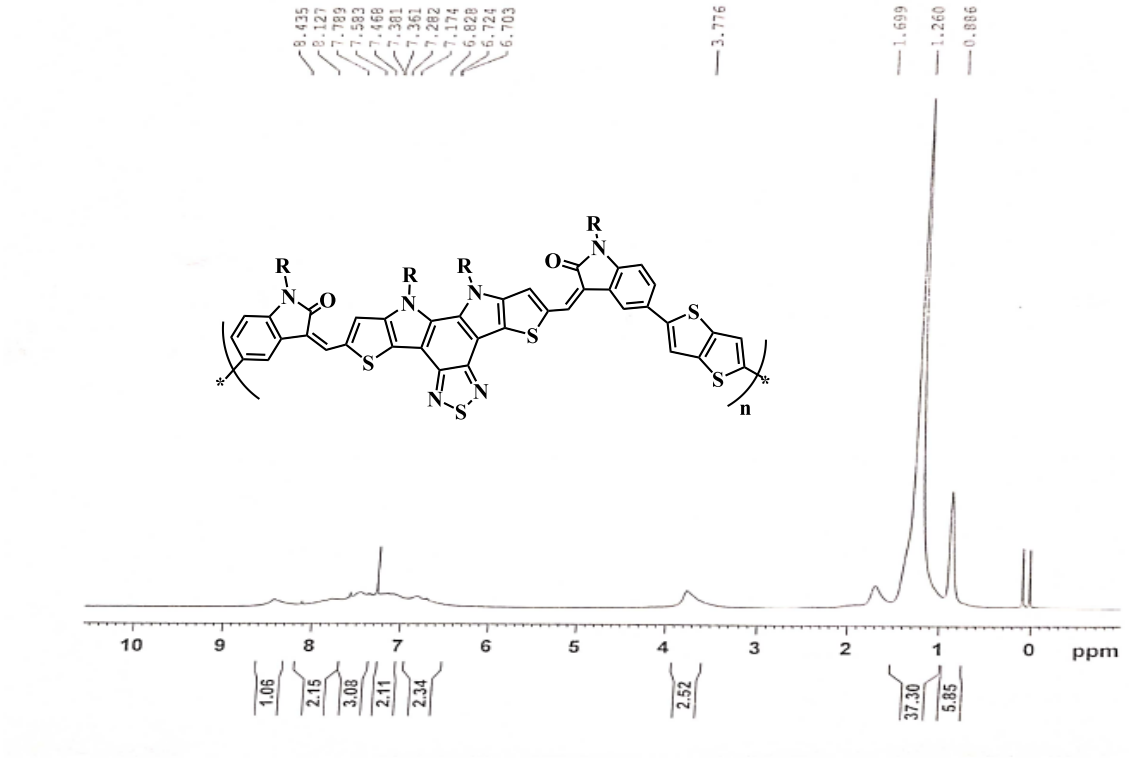

Figure 3.33 ^{1}H NMR data of polymer **DTPBT-FTP**

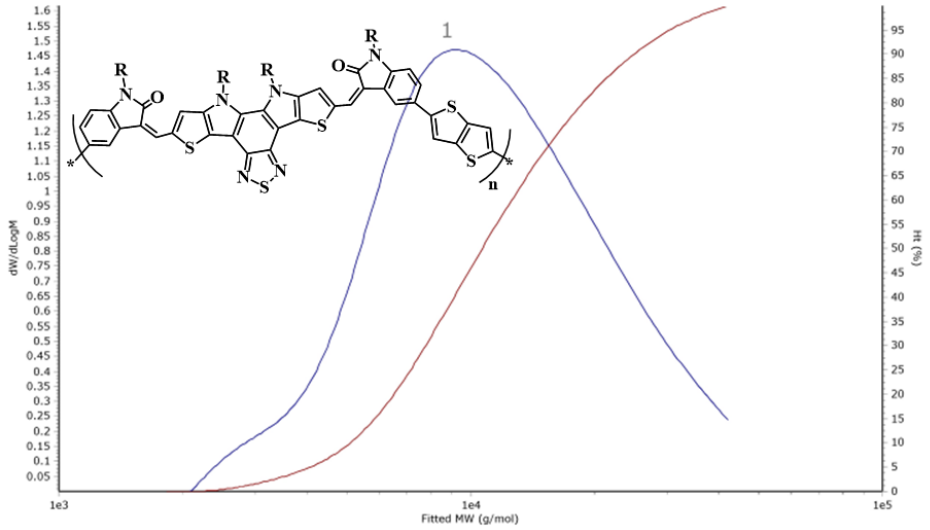

Results

Analysed by: Applied Chem at 16:52:17 on 17 December 2019

Comments

Molecular Weight Averages

Peak	Mp (g/mol)	Mn (g/mol)	Mw (g/mol)	Mz (g/mol)	Mz+1 (g/mol)	Mv (g/mol)	PD
Peak 1	9408	9120	13039	18094	23243	17327	1.43

Figure 3.34 GPC data of polymer **DTPBT-FTP**

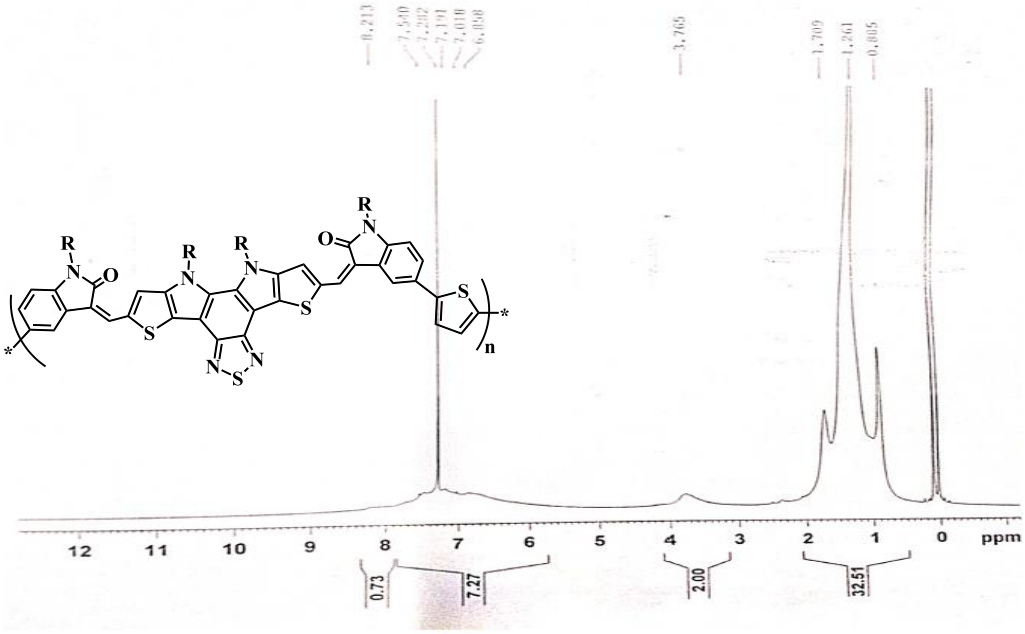

Figure 3. 35 ^{1}H NMR data of polymer **DTBT-TP**

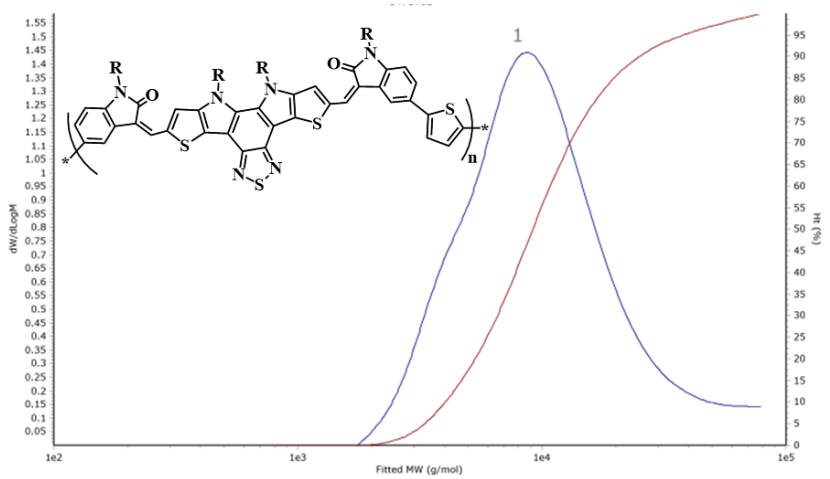

Results

Analysed by

Comments

Applied Chem at 16:37:52 on 11 April 2023

Molecular Weight Averages

Peak	Mp (g/mol)	Mn (g/mol)	Mw (g/mol)	Mz (g/mol)	Mz+1 (g/mol)	Mv (g/mol)	PD
Peak 1	8833	7743	12888	24195	40471	22063	1.664

Figure 3.36 GPC data of polymer **DTBT-TP**

References

1 J. S. Lan, L. Liu, R. F. Zeng, Y. H. Qin, Y. Liu, X. Y. Jiang, A. Aihemaiti, Y. Ding, T. Zhang and R. J. Y. Ho, *Chem. Commun.*, 2020, **56**, 1219–1222.

2 S. Wang, J. Xu, W. Wang, G. J. N. Wang, R. Rastak, F. Molina-Lopez, J. W. Chung, S. Niu, V. R. Feig, J. Lopez, T. Lei, S. K. Kwon, Y. Kim, A. M. Foudeh, A. Ehrlich, A. Gasperini, Y. Yun, B. Murmann, J. B. H. Tok and Z. Bao, *Nature*, 2018, **555**, 83–88.

3 L. Hou, X. Zhang, G. F. Cotella, G. Carnicella, M. Herder, B. M. Schmidt, M. Pätzel, S. Hecht, F. Cacialli and P. Samorì, *Nat. Nanotechnol.*, 2019, **14**, 347–353.

4 Y. Kim, C. Park, S. Im and J. H. Kim, *Sci. Rep.*, 2020, **10**, 1–12.

5 S. Roy and C. Chakraborty, *J. Mater. Chem. C*, 2019, **7**, 2871–2879.

6 E. K. Solak and E. Irmak, *RSC Adv.*, 2023, **13**, 12244–12269.

7 H. Wu, L. Ying, W. Yang and Y. Cao, *Chem. Soc. Rev.*, 2009, **38**, 3391–3400.

8 J. S. Wu, S. W. Cheng, Y. J. Cheng and C. S. Hsu, *Chem. Soc. Rev.*, 2015, **44**, 1113–1154.

9 E. H. Jung, H. Ahn, W. H. Jo, J. W. Jo and J. W. Jung, *Dye. Pigment.*, 2019, **161**, 113–118.

10 N. Y. Kwon, H. Kang, S. H. Park, H. J. Kim, C. Y. Kim, S. Park, M. J. Cho and D. H. Choi, *Dye. Pigment.*, 2020, **179**, 108391.

11 E. Wang, L. Hou, Z. Wang, S. Hellström, W. Mammo, F. Zhang, O. Inganäs and M. R. Andersson, *Org. Lett.*, 2010, **12**, 4470–4473.

12 M. Walter, F. Friess, M. Krus, S. M. Hassan Zolanvari, G. Grün, H. Kröber and T. Pretsch, *Polymers (Basel).*, 2020, **12**, 1–23.

13 Y. J. Cheng, Y. J. Ho, C. H. Chen, W. S. Kao, C. E. Wu, S. L. Hsu and C. S. Hsu, *Macromolecules*, 2012, **45**, 2690–2698.

14 Y. Liu, F. Wu, B. Zhao and P. Shen, *Eur. Polym. J.*, 2016, **74**, 180–189.

15 Y. Liu, F. Wu, B. Zhao and P. Shen, *Eur. Polym. J.*, 2016, **74**, 180–189.

16 H. E. Katz, Z. Bao and S. L. Gilat, *Acc. Chem. Res.*, 2001, **34**, 359–369.

17 F. Garnier, *Acc. Chem. Res.*, 1999, **32**, 209–215.

18 H. Sirringhaus, N. Tessler and R. H. Friend, *Science (80-.).*, 1998, **280**, 1741–1744.

19 Y. Deng, B. Sun, Y. He, J. Quinn, C. Guo and Y. Li, *Angew. Chemie - Int. Ed.*, 2016, **55**, 3459–3462.

20 M. Shaker, B. Park, J. H. Lee, W. Kim, C. K. Trinh, H. J. Lee, J. W. Choi, H. Kim, K. Lee and J. S. Lee, *RSC Adv.*, 2017, **7**, 16302–16310.

21 O. K. Kwon, J. H. Park, D. W. Kim, S. K. Park and S. Y. Park, *Adv. Mater.*, 2015, **27**, 1951–1956.

22 G. Gualtieri, S. J. Geib and D. P. Curran, *J. Org. Chem.*, 2003, **68**, 5013–5019.

23 D. Tyler McQuade, A. E. Pullen and T. M. Swager, *Chem. Rev.*, 2000, **100**, 2537–2574.

24 J. Z. Patel, T. J. Nevalainen, J. R. Savinainen, Y. Adams, T. Laitinen, R. S. Runyon, M. Vaara, S. Ahenkorah, A. A. Kaczor, D. Navia-Paldanius, M. Gynther, N. Aaltonen, A. A. Joharapurkar, M. R. Jain, A. S. Haka, F. R. Maxfield, J. T. Laitinen and T. Parkkari, *ChemMedChem*, 2015, **10**, 253–265.

25 C. Wang, H. Dong, W. Hu, Y. Liu and D. Zhu, *Chem. Rev.*, 2012, **112**, 2208–2267.

26 H. H. Fong, V. A. Pozdin, A. Amassian, G. G. Malliaras, D.-M. Smilgies, M. He, S. Gasper, F. Zhang and M. Sorensen, *J. Am. Chem. Soc.*, 2008, **130**, 13202–13203.

27 R. Mondal, S. Ko, E. Verploegen, H. A. Becerril, M. F. Toney and Z. Bao, *J. Mater. Chem.*, 2011, **21**, 1537–1543.

28 Y. Wu, Z. Li, X. Guo, H. Fan, L. Huo and J. Hou, *J. Mater. Chem.*, 2012, **22**, 21362–21365.

29 V. J. Bhanvadia, H. K. Machhi, S. S. Soni, S. S. Zade and A. L. Patel, *Polymer (Guildf).*, 2020, **211**, 123089.

30 K. Rakstys, C. Igci and M. K. Nazeeruddin, *Chem. Sci.*, 2019, **10**, 6748–6769.

31 P. J. S. Rana, R. K. Gunasekaran, S. H. Park, V. Tamilavan, S. Karuppanan, H. J. Kim and K. Prabakar, *J. Phys. Chem. C*, 2019, **123**, 8560–8568.

32 Y. J. Cheng, C. H. Chen, Y. J. Ho, S. W. Chang, H. A. Witek and C. S. Hsu, *Org. Lett.*, 2011, **13**, 5484–5487.

33 V. S. Kadam, P. A. Bhatt, H. K. Machhi, S. S. Soni, S. S. Zade and A. L. Patel, *Nano Sel.*, 2020, **1**, 491–498.

34 B. Carsten, J. M. Szarko, L. Lu, H. J. Son, F. He, Y. Y. Botros, L. X. Chen and L. Yu, .

35 Y. J. Cheng and T. Y. Luh, *J. Organomet. Chem.*, 2004, **689**, 4137–4148.

36 V. J. Bhanvadia, A. Choudhury, P. K. Iyer, S. S. Zade and A. L. Patel, *Polymer (Guildf).*, 2020, **210**, 123032.

37 V. S. Kadam, H. K. Machhi, S. S. Soni, S. S. Zade and A. L. Patel, *New J. Chem.*, , DOI:10.1039/d2nj00124a.

38 W. Zhang, N. Zheng, C. Wei, J. Huang, D. Gao, K. Shi, J. Xu, D. Yan, Y. Han and G. Yu, *Polym. Chem.*, 2016, **7**, 1413–1421.

39 A. J. Payne and G. C. Welch, *Org. Biomol. Chem.*, 2017, **15**, 3310–3319.

40 M. Zhang, X. Guo, X. Wang, H. Wang and Y. Li, *Chem. Mater.*, 2011, **23**, 4264–4270.

41 F. Babudri, G. M. Farinola and F. Naso, *J. Mater. Chem.*, 2004, **14**, 11–34.

42 Y. Li, *Oganic Optoelectronic Materials*, 2015.

43 C. Liu, K. Wang, X. Gong and A. J. Heeger, *Chem. Soc. Rev.*, 2016, **45**, 4825–4846.

44 J. Cao, X. Luo, S. Zhou, Z. Wu, Q. Zhao, H. Gu, W. Wang, Z. Zhang, K. Zhang, K. Li, J. Xu, X. Liu, B. Lu and K. Lin, *Int. J. Mol. Sci.*, , DOI:10.3390/ijms24032219.

45 K.-T. Wong, T.-C. Chao, L.-C. Chi, Y.-Y. Chu, A. Balaiah, S.-F. Chiu, Y.-H. Liu and Y. Wang, *Org. Lett.*, 2006, **8**, 5033–5036.

46 B. A. D. Neto, A. S. Lopes, G. Ebeling, R. S. Goncalves, V. E. U. Costa, F. H. Quina and J. Dupont, *Tetrahedron*, 2005, **61**, 10975–10982.

47 B. J. Schwartz, *Annu. Rev. Phys. Chem.*, 2003, **54**, 141–172.

48 B. Zhang, H. Wu, Z. Wang, A. Qin and B. Z. Tang, *J. Mater. Chem. C*, 2020, **8**, 4754–4762.

49 H. Wu, Y. Chen, X. Ling, W. Yuan, B. Li and Z. Zhou, *J. Mol. Liq.*, 2021, **329**, 115465.

50 Varun, Sonam and R. Kakkar, *Medchemcomm*, 2019, **10**, 351–368.

51 M. Jha, G. M. Shelke and A. Kumar, *European J. Org. Chem.*, 2014, **2014**, 3334–3336.

52 Z. Tribak, A. Haoudi, Y. Kandri Rodi, H. Elmsellem, M. K. Skalli, Y. Ouzidan, A. Mazzah and E. Essassi, *Moroccan J. Chem. Z. Tribak/ Mor. J. Chem. Mor. J. Chem. Mor. J. Chem*, 2016, **4**, 1157–1163.

53 S. Xu, Y. Liu, J. Li, Y. Wang and S. Cao, *Polym. Adv. Technol.*, 2010, **21**, 663–668.

54 C. Kitamura, S. Tanaka and Y. Yamashita, *Chem. Mater.*, 1996, **8**, 570–578.

55 S. I. Kato, T. Furuya, A. Kobayashi, M. Nitani, Y. Ie, Y. Aso, T. Yoshihara, S. Tobita and Y. Nakamura, *J. Org. Chem.*, 2012, **77**, 7595–7606.

56 S. Edition, W. Koch and M. C. Holthausen, *Wolfram Koch , Max C . Holthausen A Chemist ' s Guide to*, 2001, vol. 3.

57 M. J. Frisch, G. W. Trucks, H. B. Schlegel, G. E. Scuseria, M. A. Robb, J. R. Cheeseman, G. Scalmani, V. Barone, B. Mennucci, G. A. Petersson, H. Nakatsuji, M. Caricato, X. Li, H. P. Hratchian, A. F. Izmaylov, J. Bloino, G. Zheng, J. L. Sonnenberg, M. Hada, M. Ehara, K. Toyota, R. Fukuda, J. Hasegawa, M. Ishida, T. Nakajima, Y. Honda, O. Kitao, H. Nakai, T. Vreven, J. A. Montgomery, J. E. Peralta, F. Ogliaro, M. Bearpark, J. J. Heyd, E. Brothers, K. N. Kudin, V. N. Staroverov, R. Kobayashi, J. Normand, K. Raghavachari, A. Rendell, J. C. Burant, S. S. Iyengar, J. Tomasi, M. Cossi, N. Rega, J. M. Millam, M. Klene, J. E. Knox, J. B. Cross, V. Bakken, C. Adamo, J. Jaramillo, R.

Gomperts, R. E. Stratmann, O. Yazyev, A. J. Austin, R. Cammi, C. Pomelli, J. W. Ochterski, R. L. Martin, K. Morokuma, V. G. Zakrzewski, G. A. Voth, P. Salvador, J. J. Dannenberg, S. Dapprich, A. D. Daniels, Farkas, J. B. Foresman, J. V Ortiz, J. Cioslowski and D. J. Fox, *Gaussian 09, Revis. B.01, Gaussian, Inc., Wallingford CT*, 2009, 1–20.

58 K. K. Sonigara, Z. Shao, J. Prasad, H. K. Machhi, G. Cui, S. Pang and S. S. Soni, *Adv. Funct. Mater.*, 2020, **30**, 1–9.